„ROLE OF THE HISTONE KINASE MSK1 ON MLL GENE REGULATION“

„THE MOLECULAR BASIS OF INHIBITORY SIGANLLING DURING NEURONAL REGENERATION“

By
MAAIKE WIERSMA

A thesis submitted to the
University of Birmingham
for the Degree of
Master of Research

Medical School
College of Medical and Dental
Sciences
University of Birmingham
August 2011

Table of Contents

Tabele of Figures

Part I

Part II

Abbreviations

The „Système International d' unités" (SI) was used.

λ	Wave length
^{o}C	Degree Celscius
ac	acetylation
ADP	Adenosindiphosphate
APS	Ammoniumpersulfate
bp	Basepairs
CBP	CREB-binding protein
cDNA	Complementary DNA
CNS	Central nervous system
CO_2	Carbon dioxide
C-terminal	Carboxy-terminal
Da	Dalton
dH_20	Distilled water
ddH_2O	Double distilled water
DNA	Deoxyribonucleic acid
DTT	Dithiothreitol
EDTA	Ethylendiamintetraacetate
EGFR	Epidermal growth factor receptor
EGTA	Ethylene glycol tetraacetic acid
ERK	Extracellular-signal-regulated kinases
FBS	Foetal Bovine Serum
Fc	Fragment, crystallizable
FCS	Foetal Calf Serum
GDP	Guanosine diphosphate
GFP	Green fluorescent protein
GPI	Glycosylphosphatidylinositol
GST	Glutathione-S-transferase
GTP	guanosine triphosphate
h	Hour
Ig	Immunoglobulin
HMT	Histone-methyl-transferase
kb	Kilobasepairs
LRR	Leucine-rich repeat

MAP	Mitogen-activated protein
MAG	Myelin-associated glycoprotein
me	methylation
MLL	mixed lineage leukemia 1
MSK1	Mitogen- and stress-activated protein kinase-1
min	Minute
NGF	Nerve growth factor
NgR	Nogo Receptor
Ni-NTA	Nickel-nitrilotriacetic acid
NR	Non-reducing conditions
N-terminal	Amino-terminal
OD_{280}	Optical density at wavelength of 280 nm
OMgp	Oligodendrocyte-myelin glycoprotein
p	phosphorylation
PCR	Polymerase chain reaction
pH	Potentia hydrogenii
PMSF	Phenylmethylsulfonylflouride
R	Reducing conditions
rmp	Rotations per minute
RNA	Ribonucleinacid
SCF	Stem Cell Factor
SDS	Sodium-dodecyl sulfate
shRNA	Shorthairpin RNA
sec	Second
TBE	Tris / boric-acid / EDTA
TE	Tris / EDTA
TEMED	N,N,N',N'-Tetramethylethylendiamin
Tris	Tris-(hydroxymethyl)-aminomethan
TSS	Transcription Start Site
Tween	Polyooyetylenesorbitanmonolaurate
U	Unit
UV	Ultraviolet
WDR5	WD repeat-containing protein 5

Part I

Project 1

„Role of the histone kinase Msk1 on MLL gene regulation“

This project is submitted in partial fulfilment of the requirements for the award of the MRes

Abstract

The mixed-lineage leukaemia (MLL) protein is a histone methyl-transferase, that deposits the trimethylation mark on Lysine 4 of Histone 3 (H3K4me3) and that is often mutated in certain forms of leukaemia. MLL is normally associated with a cohort of other proteins and cofactors, but the mechanisms regulating MLL activity remain unclear. The H3K4me3 mark, as deposited by MLL's SET domain, which is found in many proteins and mediate lysine-directed histone methylation, is asociated with actively transcribed genes. Here we examine the role of Msk1, a downstream kinase of the MAP-kinase pathway, in regulating MLL1 activity. Msk1 is known to deposit phosphorylation marks on H3 and these were found on MLL1 target genes and the same target site like MLL1. It could be demonstrated that in Msk1 knock-down cells the MLL1 target genes are down-regulated. Furthermore during the cell cycle MLL1 and Msk1 show the same varying distribution. These findings suggest that MLL1 is regulated by extracellular signals via the MAP-kinase pathway and Msk1.

1. Introduction

1.1 Epigenetic regulation

All cells of an individual have the same DNA, which carries the same genetic information. So the cell's identity is defined by its characteristic pattern of gene expression and silencing. This pattern has to be maintained through DNA replication, chromatin assembly and DNA condensation in mitosis. Furthermore it has to be passed onto daughter cells and therefore can be described as the "cellular memory" of the cell (Turner 2002). There are a variety of processes which can effect gene expression programs without altering the DNA sequence, referred as "epigenetic mechanisms" (Delcuve, Rastegar et al. 2009). In order to establish a stable heritable epigenetic state, an incoming signal from the environment needs to be translated, for example by triggering intracellular pathways, which impacts on gene expression and the chromatin environment. Finally processes are needed to sustain this chromatin state (Berger, Kouzarides et al. 2009). These processes include DNA methylation and histone post-translational modifications (Turner 2005; Berger 2007) but also others like substitution of histones with histone variants (Khorasanizadeh 2004) or alter nucleosome positioning (Henikoff 2008; Schones, Cui et al. 2008). This gives the same cells the ability to respond to stimuli in a different way and to proceed with different identities (Jaenisch and Bird 2003). Nucleosomes therefore not only compact the genome, but have a more complex function as regulators of the genome. As the epigenome can be modulated by environmental factors, including chemicals, nutrition and aging, it therefore provides an important interface between genes at the environment (Franklin and Mansuy 2010).

1.1.1 Chromatin Organisation

As shown in Figure 1.1, DNA is packaged in the nucleus by its association with histones to form chromatin, which is highly folded, constrained and compacted by histones and non-histone proteins in a dynamic polymer. Chromatin is the physiological template for all eukaryotic genetic information (Woodcock and Ghosh 2011). The basic unit of DNA packing are the histones, small basic proteins consisting of a globular domain and a flexible and

charged NH_2-terminus (Jenuwein and Allis 2001). Two copies of each histone protein (H2A, H2B, H3 and H4) are assembled into an octamer, around which 145 – 147 base pairs of DNA are wrapped in a left handed superhelix. Together they form the nucleosome core (Luger, Mader et al. 1997). This nucleoprotein complex is essentially the same in all eukaryotes, is one of the most highly conserved structures known, and is regularly repeated in the eukaryotic genome (Turner 2005).

Nucleosomes are assembled into higher-order structures, which in higher eukaryotes are stabilized by the positively charged linker histone H1, which acts to maintain the wrapping of the negatively charged DNA around the octamer (Zheng and Hayes 2003). It is known that the nucleosomes self-assemble into a "30-nm chromatin fibre", of which probably the interphase chromosomes consist of and which further condenses allowing the formation of metaphase chromosomes, where the chromatin is most compacted (Felsenfeld and Groudine 2003; Dorigo, Schalch et al. 2004).

1.1.2 Histone Modification and their read-out

As shown in Figure 1.1 The histone tails, which protrude from the core nucleosome, are the target of several covalent modifications (Turner 2005). The post-translational histone modifications act basically in two ways. They can either alter the physical properties of the histone tail or the nucleosome or they can create new epitopes or binding surfaces for histone tails and act so as a 'histone code', which can be decoded by effector proteins (Jenuwein and Allis 2001; Macdonald, Welburn et al. 2005). More than 70 different sites for histone modification and eight main types of modifications have been reported (Taverna, Li et al. 2007). They are methylation, acetylation, phosphorylation, ubiquitinylation, sumoylation, biotinylation, ADP- ribosylation and prolyl-isomerisation (Lee and Mahadevan 2009). Despite this variety, the majority of added modifications are acetyl, methyl and phosphate groups (Taverna, Li et al. 2007). Distinct modifications act to recruit chromatin-associated proteins, which result in different processes occurring in the adjacent DNA (de la Cruz, Lois et al. 2005). The many different types of post-translational modifications act to both positively and negatively regulate gene expression (Hansen, Nyborg et al. 2010). The modifications on histones are dynamic and rapidly changing. They can appear and disappear

Figure 1.1: Chromatin organisation

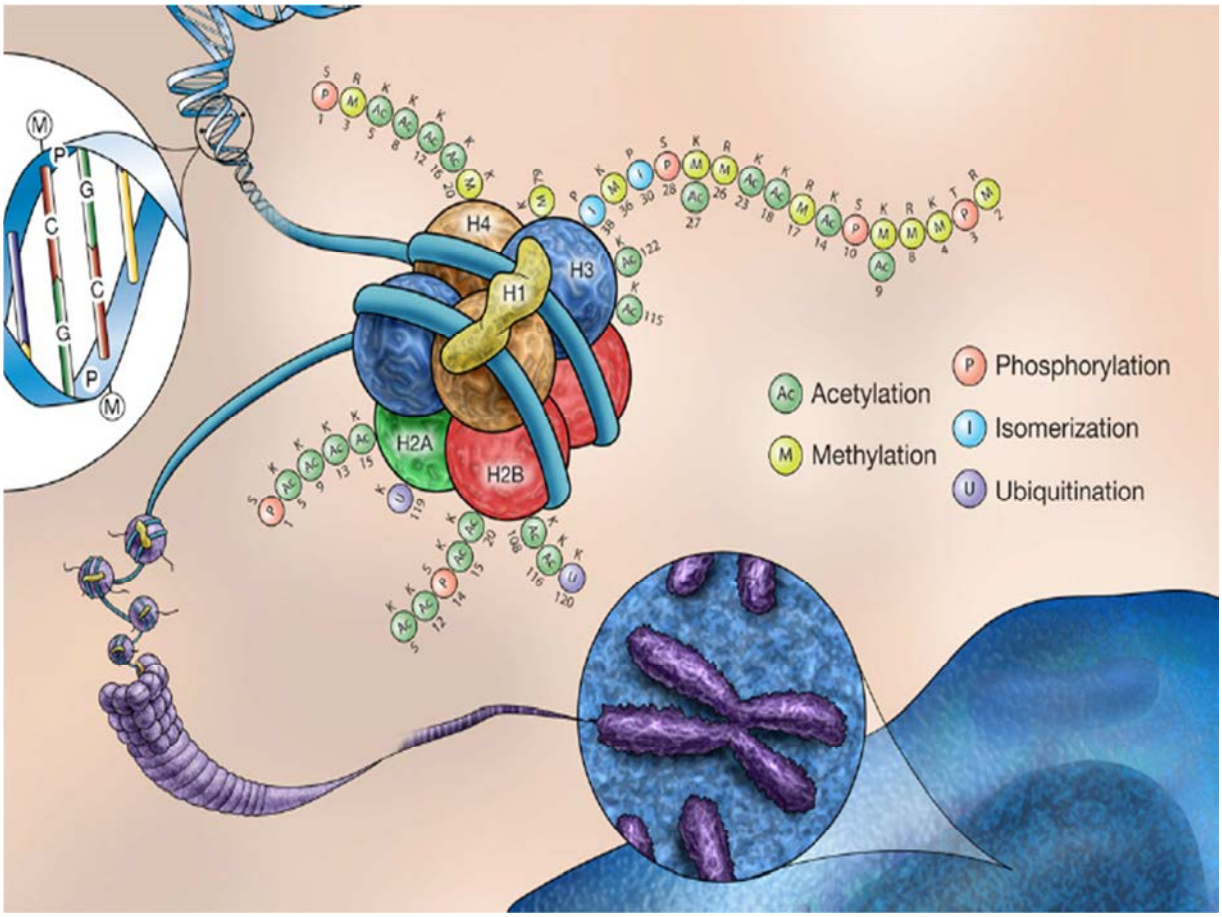

Figure 1.1: Chromatin organisation. The DNA is wrapped around the nucleosome, which consists of two copies of each of the histones H2A, H2B, H3 and H4. The DNA binding is stabilised by the linker histone H1. The nucleosome is the fundamental repeating unit of chromatin and supports further assembly into the 30-nm chromatin fibre, which can be condensed even more untill it has its most compact form during mitosis. The DNA itself can be epigeneticly modified by methylation. The histone tails, which protrude from the core nucleosome, also can be target of specific groups on distinct residues **(Baber and Rastegar, 2010).**

on chromatin within minutes of stimulus arriving at the cell surface (Kouzarides 2007). All modifications therefore require specialized chromatin modifying proteins. On one side there must be a class of enzymes which deposit the modifications and on the other side there must exist a class of enzymes, which remove these marks. Those two classes of enzymes act antagonisticly. The balance between the actions of these enzymes serves as a key regulatory mechanism for gene expression and governs numerous developmental processes and disease states (Haberland, Johnson et al. 2009). Histone modifications may regulate access to the DNA and thus influence nuclear processes. An important issue when considering 'histone-code'-modifications, is how they are translated. Histone modification marks provide highly selective binding sites for a series of effector proteins (Mellor 2006). Those effector or readout enzymes have in common, that they carry different but highly conserved domains, which recognize the modification at certain residues, and are so able to interact with chromatin and/or its modified components (Figure 1.2). The bromodomain for example functions as an acetyl-lysine binding domain (Mujtaba, Zeng et al. 2007). The members of the Royal superfamily are readers of higher lysine methylation, like for example the chromodomain. The binding affinities of chromodomains and of bromodomains to their respective modified lysines have been shown to be relatively weak, which are thought to allow for rapid 'on-off' binding (Daniel, Pray-Grant et al. 2005). PHD fingers are also highly specialized methyl-lysine binding domain and are often found in close proximity to a bromodomain (Mellor 2006). The combination of modification-binding sites may genenerate additional specifities (Taverna, Li et al. 2007). A special role has been identified for the protein 14-3-3, which recognizes phosphorylated histone residues. 14-3-3s are well-conserved and abundant phosphor specific binding proteins, which binds to phosphorylated histone H3 (Macdonald, Welburn et al. 2005).

Figure 1.2: Histone post-translational modifications and binding partners

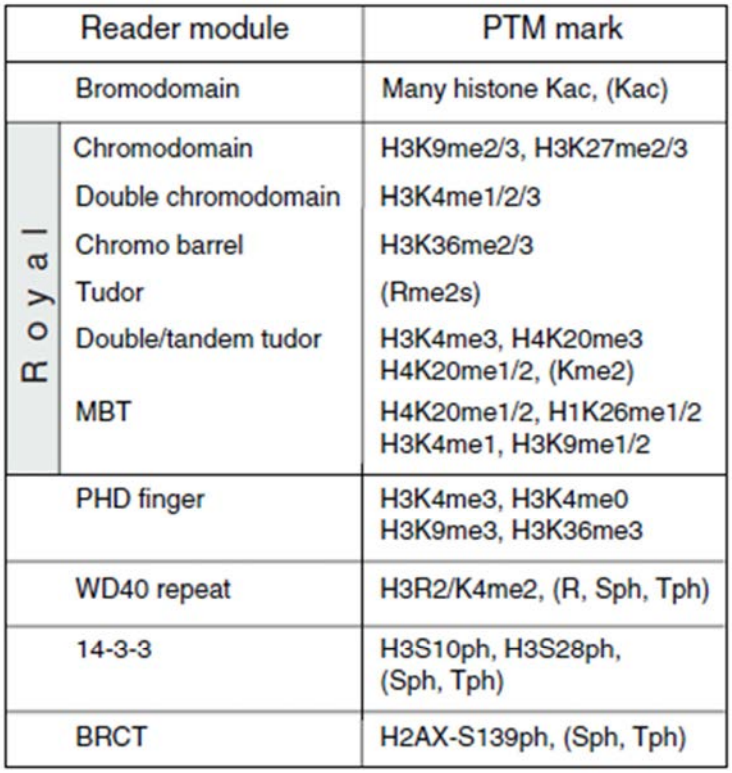

	Reader module	PTM mark
	Bromodomain	Many histone Kac, (Kac)
Royal	Chromodomain	H3K9me2/3, H3K27me2/3
	Double chromodomain	H3K4me1/2/3
	Chromo barrel	H3K36me2/3
	Tudor	(Rme2s)
	Double/tandem tudor	H3K4me3, H4K20me3 H4K20me1/2, (Kme2)
	MBT	H4K20me1/2, H1K26me1/2 H3K4me1, H3K9me1/2
	PHD finger	H3K4me3, H3K4me0 H3K9me3, H3K36me3
	WD40 repeat	H3R2/K4me2, (R, Sph, Tph)
	14-3-3	H3S10ph, H3S28ph, (Sph, Tph)
	BRCT	H2AX-S139ph, (Sph, Tph)

Figure 1.2: Histone post-translational modificatons and binding partners. In order to read the histone code, reader proteins contain specified reader modules. The shown domain groups are known chromatin-associated modules and the histone marks they have been reported to bind to. The bromodomain recognizes acetylated residues, the chromodomain recognizes methylated residues , as well as the PHD finger domain. Phosphorylated residues are recognized by 14-3-3 **(Taverna et al., 2007).**

1.1.3 "Crosstalk" between epigenetic modifications modification

Although some modifications are clearly linked with defined functions (acetylation and H3K4me3 for example with activation and H3K27me3 with silencing), the precise function of most modifications are still unknown (Lee and Mahadevan 2009). The high density of sites and various types of histone modification plus additional DNA methylation might indicate that many chromatin marks are not recognized independently and that they act together (Nightingale, Gendreizig et al. 2007). For example H3S10p is involved in two apparently opposed chromatin states (transcriptionally active decondensed euchromatin, versus condensed mitotic chromosomes and silent heterochromatin) (Fischle 2008). It is more likely, that modifications influence each other's functions. This "crosstalk" can appear in several forms and therefore chromatin modifications can enhance or block their functions. Crosstalk can occur between modifications on a single histone molecule but also between histone modifications on different histones, between histone modification and DNA methylation or between chromatin modifications on different nucleosomes (Latham and Dent 2007; Nightingale, Gendreizig et al. 2007).

1.2 A specific histone methyltransferase - MLL

MLL, the mixed-lineage leukaemia protein, is a histone methyltransferase, specific for lysine 4 of histone 3 (Yokoyama, Somervaille et al. 2005). MLL codes for a large protein of ~ 3900 amino acids, which is cleaved post-translationally into a 320 kDa N-terminus (MLL^N) and a 180 kDa C-terminus (MLL^C). The two subunits are bound non-covalently in a tight complex (Slany 2005). The domain structure, as shown in Figure 2.1 A, is complex. Two domains, FYRN and FYRC, have been found to be important for the hetero-dimerization between MLL^N and MLL^C (Ansari, Mishra et al. 2009). MLL^N contains DNA and chromatin targeting domains and a repression domain which recruits repression complexes. MLL^C contains a CBP-binding activation domain and the SET domain and is therefore responsible for the methylation of the lysine (Chen, Santillan et al. 2008). Although the MLL^N- subunit contains repressive domains, in combination with MLL^C they result in transcriptional activation (Slany 2005).

Figure 1.3: MLL domain structure and MLL-complex

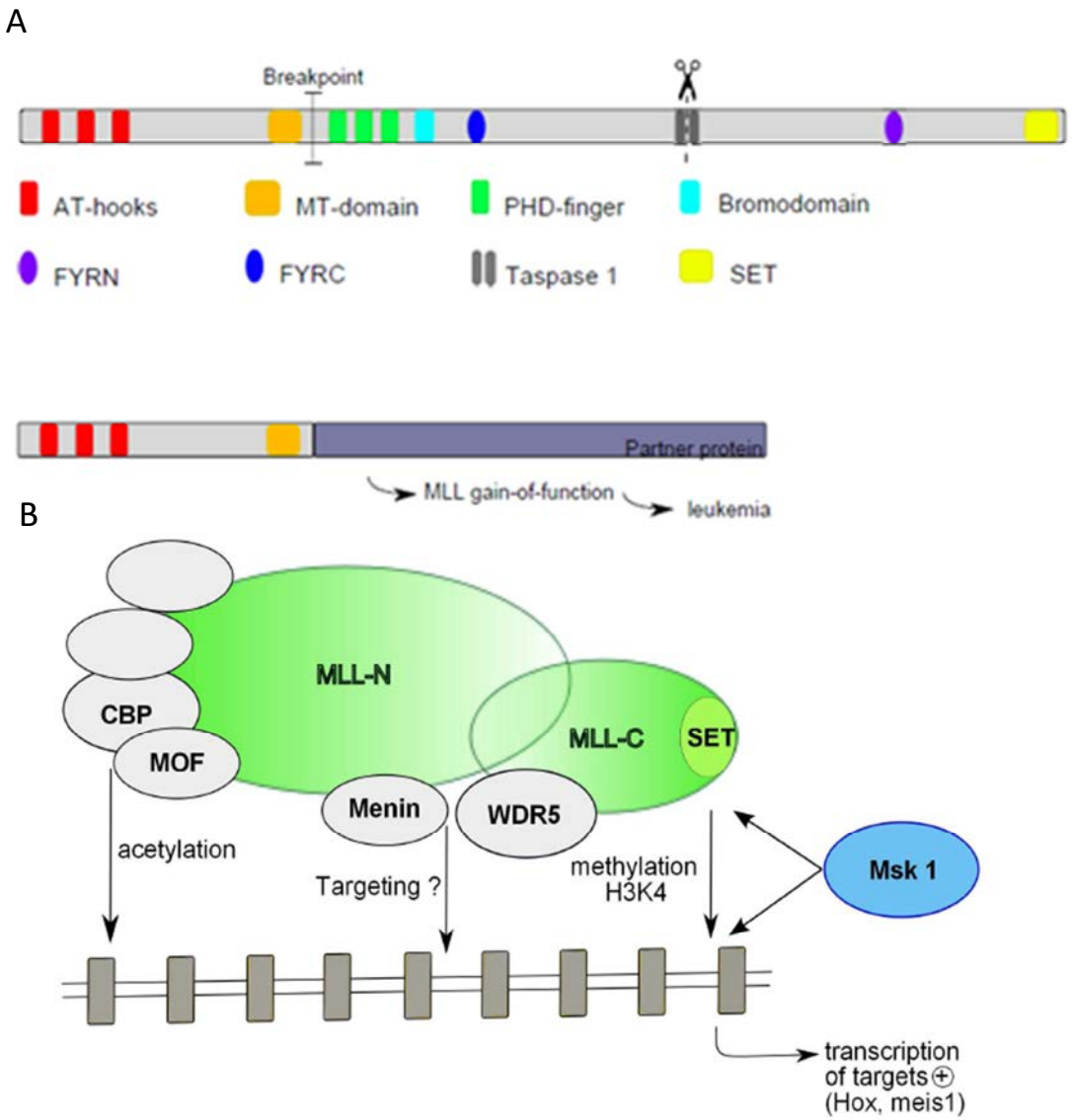

Figure 1.3: MLL domain structure and MLL-complex. (A) At the end of the N-terminus, three AT-hooks are located, followed by a MT domain with a CxxC signature. Both are involved in non-specific binding to the DNA. Close to the MT-domain, the three PHD finger cassette is found. PHDs are usually involved in protein-protein interaction, or recognition of specific methyl lysine residues. Bromodomains are involved in the recognition of acetylated lysine residues at histone tails. The histone lysine methylation activity is located at the SET domain at the C-terminus. The whole protein is post-translationally cleaved at the Taspase1 restiction site. The FYRN and FYRC domains together play roles in the association of these protein fragments as a complex. In MLL fusion proteins the C-terminal sequence is replaced by a partner protein. The partner proteins convert the truncated MLL into a potent translational activator, and leukaemia develops. (B) MLL is a large protein, that is cleaved after translation in two fragments, which are bound tightly together. MLL is associated with a cohort of other factors, so a multi-protein complex is formed. Some of the proteins are involved in binding the complex to the chromatin (WDR5=histone-binding; menin= DNA-binding). Others are modifiers of chromatin (MLL=methyltransferase; MOF; CBP=histone acetyltransferase).

Two regions have been identified within MLL^N to process the finding of target genes. At the extreme N-terminus three AT-hook motifs are present. They bind within the minor groove of the double helix and do not require a specific recognition sequence. A second DNA binding domain is the MT or methyltransferase-homology domain, which binds to non-methylated CpG dinucleotides, a feature characteristic of CpG islands in transcriptionally competent genes. MLL^N also contains a specialized zinc finger structure, termed PHD (plant homeodomain) fingers, which are adjacent to the MT region (Slany 2005). However, it is still unclear how MLL is recruited to its target promoter elements (Milne, Kim et al. 2002). In MLL1 the PHD fingers are found in close proximity to a bromodomain. This domain may target the PHD fingers and influence the specifity of their weak interaction (Mellor 2006; Wysocka, Swigut et al. 2006). There is growing evidence that the PHD fingers act as a reader of H3K4me3 and therefore may enhance binding or maintenance of gene expression (Milne, Kim et al. 2002; Chen, Santillan et al. 2008).

The transcriptional activation and HMT activity reside in the highly conserved SET domain. The SET domain proteins are the major catalytic components of a number of histone methyltransferase complexes that effect lysine methylation (Ruthenburg, Wang et al. 2006). In mammals six different Set1 homologues have been characterised: MLL1, MLL2, MLL3, MLL4, Set1A and Set1B. They all share the same enzymatic activity (H3K4 methylation) but they only share up to 30 % of sequence homology (Ansari, Mishra et al. 2009).

As shown in Figure 2.1 B, MLL is normally associated with a cohort of highly conserved cofactors to form a macromolecular complex (Yokoyama, Somervaille et al. 2005). It is still in discussion how many cofactors are exactly involved, with numbers varying from five to 29 other proteins. This reflects that not all the interactions are covalent and that it is not always clear whether the proteins are part of the complex or act on the same target site.

In the complex MLL integrates two major aspects of histone biology: acetylation and methylation (Slany 2005). Acetylation is for example provided by the members and histone acetyl transferases MOF and CBP. While CBP only interacts transiently with MLL1, MLL1 and MOF are recruited together (Dou, Milne et al. 2005). Another member of the complex WDR5 recognises dimethyl-K4 on histone 3. It is likely that WDR5 has a 'peptide presentation' role in the MLL complex involved in H3K4 trimethylation and serves to present the K4 side chain to further methylation (Ruthenburg, Wang et al. 2006). Menin, as a further member of the complex, is a positive regulator of *Hox* gene expression and is associated

with chromatin on *Hox* gene loci (Yokoyama, Somervaille et al. 2005). WDR5 and Menin play roles in recruiting the MLL complex to target loci, but the mechanisms remain unclear (Ruthenburg, Wang et al. 2006).

1.2.1 MLL and *Hox* genes

In mammals, MLL positively regulates multiple loci, including the clustered homeobox (*Hox)* genes (Milne, Kim et al. 2002). The homeobox genes are master developmental control genes that act at the top of genetic hierarchies regulating aspects of morphogenesis and cell differentiation in animals. Hox-proteins are crucial to the correct development of bilateral organisms (McGinnis, Garber et al. 1984; Hueber, Weiller et al. 2010).

The mammalian *Hox* genes are defined by virtue of their homology with the genes of the homeotic complex in *Drosophila*. There are 39 Hox genes organised in four clusters, HoxA, HoxB, HoxC and HoxD, each located on a different chromosome and comprising 9-11 genes. They encode highly conserved transcription factors with key roles in normal development (Barber and Rastegar 2010).

Hox genes also play a key role in hematopoietic differentiation (Milne, Kim et al. 2002). Gene expression analyses of both mouse and human bone marrow samples revealed that the majority of *Hox* genes of the A, B and C clusters are expressed temporally during haemopoietic differentiation. The MLL methyl-transferase is required for the proper maintenance of *Hox* gene expression during development. In mouse MLL plays an essential role in definitive hematopoiesis by inducing the proliferation and differentiation of hematopoietic progenitors through the maintenance of *Hox* gene expression (Argiropoulos and Humphries 2007). MLL regulates specific *Hox* target loci by direct binding, which modulates levels of histone H3 lysine 4 methylation by targeting the intrinsic SET domain to the promoters. But how MLL regulates *Hox* gene expression is poorly understood (Milne, Kim et al. 2002).

During embryogenesis, MLL is required for maintenance of *Hox* gene expression to establish proper body segment identity. In the hematopoietic compartment, lack of MLL is associated with reduced expansion of progenitors and decreased *Hox* gene expression. Conversely, hematopoietic cells transformed by MLL oncoproteins consistently hyperexpress several *Hoxa* cluster genes as well as the Meis1 gene, some of which have been shown to be direct

targets of MLL and key contributors to the pathologic features of MLL associated leukaemia (Yokoyama, Somervaille et al. 2005).

1.2.2 MLL in the context of histone modifications

Histone modifications are not deposited or recognized in isolation but comprise a complex and inter-related collection of modifications at adjacent residues. H3 lysine 4 methylation is involved in gene activation and functionally linked with histone H3 acetylation. H3 acetylation can either facilitate the rate and/or the processivity of HMTase activity or act by inhibiting the action of a putative H3K4me3 demethylase. It has been shown, that MLL1's SET1 domain is stimulated in vitro by substrate acetylation (H3K9) together with phosphorylation at H3S10 (Nightingale, Gendreizig et al. 2007).

H3 phosphorylation appears only on a subfraction of nucleosomes and is elicited by ERK and p38 MAP kinases, which act through their downstream kinases Msk1/2 (as show in Figure 2.2). In Msk knock-down cells, an almost complete loss of histone phosphorylation was observed (Soloaga, Thomson et al. 2003). Phosphorylation appears at conserved serines on histone H3 and H4, but still little is known about histone phosphorylation and gene expression. However it was demonstrated that H3 phosphorylation is concomitant with early gene induction directly after extracellular stimuli by initiating intracellular signalling that rapidly elicit transcription of a subset of genes in the nucleus (Thomson, Clayton et al. 1999). Beside the correlation of H3 phosphorylation and the induction of immediate-early (IE) genes, H3 phosphorylation is also reported in conjunction with other inducible genes and oncogenes (Dyson 2005).

MAPKs (mitogen-activated protein kinase), are a family of evolutionarily conserved enzymes, which regulate eukaryotic gene expression in response to extracellular stimuli, like cytokines, growth factors and cellular stress.

Figure 1.4: Ras-MAPK-MSK pathway and the nucleosomal response

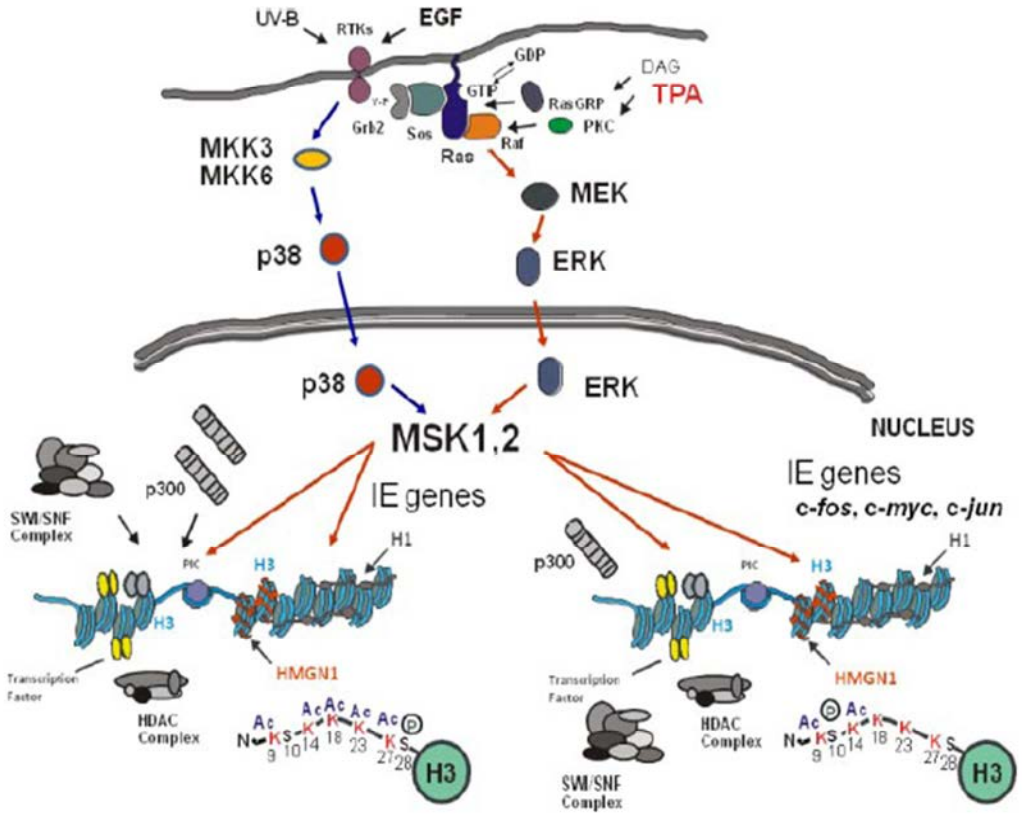

Figure 1.4: Ras-MAPK-MSK pathway and the nucleosomal response. Extracellular stimuli , like UV irradiation or treatment with growth factors (EGF), trigger intracellular pathways, which can activate either the p38 or ERK kinases. Both kinases can activate the mitogen and stress activated protein kinases 1 and 2 (Msk1 and Msk2), which leads to phosphorylation of histone H3 and the activation of immediate early (IE) genes. It is been suggested, that H3 phosphorylation is a key event linking the MAPK signaling cascade with chromatin remodeling **(Decuve et al., 2009).**

MAPKs, in context with their downstream kinases, in general phosphorylate transcription factors, co-regulators and chromatin proteins to initiate transcriptional changes. They are able to form integral components of transcription complexes, act as enzymatically functioning structural adaptors, involved in the phosphorylation of local substrates and recruitment of chromatin-remodelling complexes, other transcription factors and the general transcription machinery (Widmann, Gibson et al. 1999).

In mammals at least four parallel MAPK cascades exist, that respond to distinct extracellular stimuli. H3 phosphorylation is triggered by cascades under the influence of ERK and p38. There is evidence for a link between the MAPK cascade and chromatin modification during gene induction. MAPKs can provide indirect routes that localize nucleosomal modification at inducible genes (for example promoting association of histone acetyl-transferases with transcription factors in a phosphorylation-dependent manner) (Edmunds and Mahadevan 2004). It is been suggested that H3 phosphorylation is a key event linking the MAPK signalling cascade with chromatin remodelling (Delcuve, Rastegar et al. 2009).

Msk phosphorylates H3 at serine 10 and 28 and these marks are targeted to different genetic loci and are likely to underpin different functions at these positions. But why? Msk does not have an intrinsic specifity for one residue because in vitro they phosphorylate both residues. Maybe there is a local restriction of the kinase in vivo to one or the other class of loci, where the kinase and other proteins build a complex, so that only one site is available. It is also possible, that Msk activity is modulated, by the interaction within different complexes, which provides a mechanism to target site specific modifications to particular loci (Dyson, Thomson et al. 2005). Nevertheless, Msk mediated H3 phosphorylation is a crucial intermediate step between signalling at cell-surface receptors and transcriptional reprogramming and it has been suggested that H3 phosphorylation leads to chromatin remodelling, giving transcription factors access to regulatory DNA sequences (Drobic, Perez-Cadahia et al. 2010). Recently it has been demonstrated that Msk1 targeting to the endogenous c-fos promoter is sufficient to activate its expression without the need of upstream signaling. Moreover, targeting Msk1 to the α-globin promoter induces H3 S28 phosphorylation and reactivates expression of polycomb-silenced genes (Lau and Cheung 2010).

Subsequent studies on the modifying enzymes responsible for generating MLL stimulating marks (H3K9ac/S10p) indicate that the histone H3S10 specific kinase Msk1 is present at MLL

target loci (*Hoxa*-loci) (unpublished data). Furthermore Msk1 is a potential component of the MLL1 complex. Together this suggests that Msk1 dependant histone H3S10 phosphorylation contributes to the regulation of MLL methyltransferase activity at *Hoxa*-genes. It is hypothesised that this is a key means of regulating MLL activity under normal conditions, and that this regulatory mechanism is disrupted by MLL fusion proteins, which occur in certain types of leukaemia (Lab Nightingale, data not published).

1.3 Aims

Msk1 (Mitogen- and Stress- activated Protein Kinase 1) is a protein kinase involved in the phosphorylation of H3S10 (Soloaga *et al.*, 2003), but is also downstream of the MAP-kinase signalling pathway (Edmunds and Mahadevan, 2004; Huang *et al.*, 2006). Previous data from the lab (not published) suggest that H3S10p contributes to Hoxa gene activation. Furthermore the sites of Msk1 binding correlated with the modifications deposited by proteins of the MLL complex. The data suggested that Msk1 is either part of the MLL complex or acted together with the MLL complex to regulate *Hoxa* gene expression. In this project the role of Msk1 on the regulation of MLL1 target genes should be explored. Therefore a knock-down in HPC-7 cells needs to be established and the effect of the down regulation on known MLL target genes should been examined. To explore the interaction of Msk1 and MLL1 Co-IPs were performed. Furthermore it should be investigated how Msk1 and MLL1 may be involved and therefore a co-localisation study was carried out, which led to investigation of cell-cycle dependet changes in Msk1 abundance.

2. Materials and Methods

2.1 Tissue Culture

2.1.1 Cultivation of HPC7 cells

HPC7 cells are an immortalised Mouse Embryonic Stem Cell (ESC-like) line (Pinto Do *et al.*, 1998). HPC7 cells have the capacity to differentiate into several different cell types, notably into megakaryocytes, using thrombopoietin (TPO, Peprotech) or monocytes (IL3 and IL6, Proprotech).

Cells were grown in "HPC7 Growth Medium". Cells were counted every day and diluted to $1x10^6$ cells per ml in growth medium with recombinant SCF (100 ng/µl, used 1 µl per 1 ml medium, Vitrolife). Every second day the medium was replaced with fresh medium. The cells were kept at 37°C and 5% CO_2.

HPC7 Growth Medium: StemPro-34 SFM medium
StemPro-34 Nutrient Supplement (Invitrogen)
1/100 penicillin (10000 U/ml) (Gibco)
1/100 streptomycin (10000 µl/ml) (Gibco)
1/100 L-glutamine (200 mM) (Invitrogen)

2.1.2 Cultivation of LCL cells

LCLs are a human lymphoblastoid cell line with a normal karyotype. The cells were grown in RPMI medium. After three to four days, dependent on their density, the cells were splitted 1:4 and set into fresh medium and kept at 37°C and 5% CO_2.

RPMI Medium: Gibco RPMI 1640 Medium
1/100 penicillin (10000 U/ml) (Gibco)
1/100 streptomycin (10000 µl/ml) (Gibco)
1/100 L-glutamine (200 mM) (Invitrogen)
50 ml Fetal Bovine Serum (Invitrogen)

2.1.3 Arrest of cells in the Cell Cycle

In order to arrest cells at certain points in the cell cycle thymidine (Sigma) and colcemid (Gibco) were used. Thymidine was added to the medium of the cells in a final concentration of 1mM and incubated for 15 hours. It inhibits the cell cycle during S-phase. Colcemid was added to the medium of the cells in a final concentration of 0.1 µg/ml and incubated for 15 hours. It inhibits the cell cycle during at G_1-M.

2.2 Protein Methods

2.2.1 Preparation of whole cell extract

Cells were collected and washed three times with ice-cold PBS before the cell pellet was resuspended in 500 µl Lysis buffer. The mixture was left on a rotating wheel at 4°C for 30 minutes. The mixture was sonicated at high amplitude for 1 minute and afterwards centrifuged at 13000 rpm for 10 minutes at 4°C. The supernatant was kept.

PBS: 2.7 mM KCl
137 mM NaCl
8.1 mM Na_2HPO_4
1.76 mM KH_2PO_4, pH 7.4

Lysis Buffer: 10 mM Tris, pH 8
150 mM NaCl
5 mM EDTA
0.5 mM EGTA
1 mM β-Mercaptoethanol
1% Nonidet P40
25% Glycerol
1 tablet protease inhibitor (Roche) per 10 ml
10 µl PMSF per 10 ml

2.2.2 Sodium dodecyl sulphate polyacrylamide gel electrophoresis (SDS-PAGE)

Proteins were separated according to size (Laemmli, 1970). The samples were loaded on an acrylamide gel, with a concentration dependent on the size of the proteins to be separated. For the detection of Msk1 (~90 kDa MW) and Actin (~50 kDa MW) a 15% SDS gel was prepared. The resolving gel was overlaid with 70% ethanol. The ethanol was removed before the stacking gel was prepared on top of the resolving gel. Protein samples were resuspended in SDS Loading buffer, incubated at 100°C for 10 minutes and loaded onto the gel. The gel was electrophoresed at 200 V, 300 mA and 20W, for three hours in a standard vertical electrophoresis unit.

10% SDS gel: 15ml Bis-acrylamide (30%Acrylamide-0.8% Bis)
250 µM Tris-HCl, pH 8.8
300 µl 10% SDS
100 µl 10% Ammonium Persulfate
30 µl TEMED made up to 30 ml with distilled water

stacking gel: 1 ml Bis-acrylamide (30% Acrylamide-1.6% Bis)
250 µM Tris-HCl, pH 6.8
100 µl 10% SDS
100 µl 10% Ammonium Persulfate
10 µl TEMED made up to 10 ml with distilled water

SDS reservoir buffer: 50 mM Tris
0.384 M glycine
0.1% SDS

10x SDS Gel Loading Buffer: 20% SDS
500 mM Tris, pH 7.6
50% Glycerol
1 M DTT
Bromophenol Blue

2.2.3 Immuno-detection of proteins on nitrocellulose membranes ("Western Blot")

The separated proteins were transferred (Towbin et al., 1979) onto a Hybond-C nitrocellulose membrane (Amersham) for three hours (180V/300mA/20W) using transfer buffer. The efficiency of transfer was checked by Ponceau Red staining. The membrane was incubated for one hour or overnight at 4°C in Blocking Buffer. Primary antibodies were obtained from commercial sources and are listed below. The membrane was then incubated with a first antibody (rabbit or mouse) diluted in 10% milk + 1xPBS + 0.1% Tween for 1 hour at room temperature in recommended dilutions. The membrane was washed three times, each for 15 minutes, with 10% milk + 1xPBS + 0.1% Tween. The secondary antibody (Licor 800 nm-conjugated, anti-rabbit or anti-mouse) was added in a dilution of 1/1000 in 10% milk + 1xPBS + 0.1%Tween. Binding was visualised by using the "Odyssey" (Li-Cor) imaging system. At 800nm the secondary Licor- Antibody chromophore is acitvated, permitting detection.

Transfer buffer:	25 mM Tris
	192 mM glycine
	20% methanol
Blocking Buffer:	10% dried milk powder
	1 x PBS
	0.1% Tween-20

Antibody	Source	Dilution/ Animal
α-Msk1	Abcam ab82194	1:500 / rabbit
α-beta Actin	Abcam ab8227-50	1:1000 / rabbit
Licor 2nd, α-rabbit IgG	Rockland 611-131-121	1:1000 / goat
Licor 2nd, α-mouse IgG	Rockland 610-131-121	1:1000 / goat

Table 2.1: Antibodies used for western blot

2.2.4 Transfection of HPC7 cells

The knockdown vector for Msk1 (shRNA_mir vector, Open BioSystms) was transfected into HPC7 cells using a commercial procedure (Cell Line Nucleofector® Kit L, Lonza). A 12-well plate was prepared with 1 ml of 2x HPC7 growth medium and 400 µl unsupplemented StemPro medium per well. $2x10^6$ cells were required per nucleofection and per well. The Lonza Nucleofector Kit was used as the manufacturer's instructions. Cells were centrifuged at 1200 rpm, for 10 min at room temperature and afterwards resuspended in 100 µl of Nucleofector Solution L. 2 µg of DNA was added per cell suspension, a plasmid expressing GFP (part of the kit) was used as control. The cell suspension was transferred into an appropriate cuvette for transfection with the Nucleofector™ II (programme X-001). 500 µl of pre-warmed RPMI 1640 medium (Gibco) were immediately added after transfection. The cells were then transferred into an Eppendorf tube and left 30 minutes to an hour at 37°C to recover. The cells were finally transferred into pre-warmed 12-well plate and incubated for the required time period.

2x HPC7 growth medium:	11.56 ml StemPro34 SFM medium supplemented with StemPro34 Nutrient Supplement (Invitrogen), 1/50 penicillin/streptomycin (Gibco) 1/50 glutamine (Invitrogen) 13 µl recombinant SCF (Vitrolife)

2.3 Functional Analysis

2.3.1 RNA extraction (Qiagen Kit)

Total RNA was isolated from HPC7 cells using the QIAGEN Kit (RNase free DNase Set and RNeasy® Minikit) according to the manufacturer's instructions. RNA was quantified using an UV/visible spectrophotometer (260 nm, 280 nm).

2.3.2 Real-Time Quantitative PCR (RTQ/PCR) with Reverse Transcription

This method allowed simultaneous RNA reverse transcription and cDNA amplification in one step and was performed according to the manufacturer's instructions. The reaction was achieved with commercial primers for Msk1 and Actin. The mix per tube contained the following: 5 µl of QuantiTech™ Sybr® Green Mix (Qiagen), 0.1 µl of RT-mix (Qiagen), 1 µl of primers (Qiagen, Msk1 QT00141554, Act QT01336772), 50 ng RNA template, diluted to 10 µl with water. Three analyses were performed for each sample. A control was performed without RT-mix, also in triplicate, in order to ensure the non-contamination of the products. The samples were loaded in a 384-well optical reaction plate. The RT-qPCR was performed on the 7900 HT machine (Applied Biosystems). The programme was set up as following: reverse transcription was achieved by heating the samples at 50°C for 30 minutes. The samples were then heated at 95°C for 15 minutes, 94°C for 15 seconds for denaturation, 55°C for 30 seconds for annealing, 72°C for 40 seconds for elongation. The three last steps were performed 40 times. Real time PCR employed the characteristics of a fluorescent dye, SYBR® Green, which binds to double-strand DNA. PCR products are thus visualized and quantified after each cycle of amplification, due to the emission of fluorescence by the SYBR® Green.

2.3.3 Immunoflouresense Microscopy

For microscopy, HPC7 and LCL cells were used. They were harvested by centrifuging at 1200 rpm for 5 minutes at 4°C, washed three times with ice-cold PBS and counted. The cells were diluted to a concentration of $1x10^5$cells/ml in KCM. Ethanol washed slides were fixed in chambers for the Cytospin. 200 µl of cells were put in the loading chambers and spun down for 10 minutes at 1000 rpm at room temperature. The slides with the cells were incubated in a bath of KCM for 10 minutes, before incubating with the primary antibodies. The antibodies were diluted to the recommended concentration with KCM + 0.1% BSA. The slides were stored in a humidified chamber in the fridge for one hour. After incubation the slides were washed twice in a bath of KCM for 5 minutes. They were incubated with the secondary antibody (FITC-α-rabbit IgG and TRITC-α-mouse IgG) in a 1:50 dilution. They were stored in a humidified chamber in the fridge for another hour. The slides were washed again twice in a bath of KCM for 5 minutes. For fixing the cells the slides were incubated in a bath of 4 % formaldehyde/KCM for 10 minutes. Afterwards they were washed with dH_2O. Finally, slides were mounted with 7.5 µl of a 1µg/ml DAPI in Vectorshield solution and ethanol washed coverslips and sealed.

KCM: 120 mM KCl
20 mM NaCl
10 mM Tris/HCl pH 8
0.5 mM EDTA
0.1 % Triton X-100

Antibody	Source	Dilution/ Animal
α-Msk1	Abcam ab 82194	1:1000 / rabbit
α-$MLL1^N$	Millipore 05-764	1:1000 / mouse
FITC 2^{nd}, α-rabbit IgG	Abcam ab6717	1:1000 / goat
TRITC 2^{nd} ,α-mouse IgG	Dako R0270	1:1000 / goat

Table 2.2: Antibodies used for immunoflouresence microscopy

2.3.4 Flow Cytometry Analysis

Per Analysis 50,000 – 100,000 cells were collected by centrifugation (1200 rpm, 5 min). The supernatant was discarded and the cell pellet was resuspended in 3 ml of ice-cold PBS and centrifuged again at 1200 rpm for 5 min. The supernatant was discarded and the cell pellet resuspended in 1 ml of cold 80% Ethanol/PBS. The samples were stored overnight in the freezer. After the incubation cells were centrifuged (800 rpm, 10 min) and resuspended in 1 ml ice-cold PBS. After another spin (800 rpm, 10 min) the cells were resuspended in 100 µl PBS per $5x10^4$ cells. To this 20 µl propidium iodide (concentration 5 mg/ml) per ml PBS is added and incubated for 30 - 60 minutes. The samples were then measured.

2.3.5 Co- Immunoprecipitation

Co-Immunoprecipitation was performed on LCL cells. $1x10^8$ cells were collected and washed twice in ice-cold PBS, to which 5 mM sodium-butyrate was added. The final cell pellet was resuspended in 300 µl NP40 buffer with 150 mM NaCl. The mixture was vortexed and incubated on ice for 20 min for cell lysis. The lysate was centrifuged for 20 min at 13000 rpm and the supernatant was kept. In the meantime protein A sepharose, which was soaked overnight in NP40 buffer with 150 mM NaCl, was adjusted (50% sepharose and 50% NP40 buffer with 150 mM NaCl). In order to clear the lysate the volume was made up to 400 µl with NP40 buffer with 150 mM NaCl and 40 µl of the adjusted sepharose beads were added. The mixture was incubated on a rotating wheel at 4^oC for 30 minutes. The mixture was centrifuged (13000 rpm, 1 min) and the supernatant was kept. The lysate was incubated overnight with 20 µl of antibody at 4^oC on a rotating wheel. Then 40 µl of adjusted sepharose was added and left for 3 hours at 4^oC, before centrifuging for 3 minutes, at 3000 rpm and 4^oC. The supernatant is kept as sample S_1. The beads were washed three times with NP40 buffer with 200 mM NaCl. The beads and the samples S_1 were mixed with Laemmli-buffer and loaded on a gel and a western blot prepared afterwards.

PBS: 2.7 mM KCl
137 mM NaCl
8.1 mM Na_2HPO_4
1.76 mM KH_2PO_4, pH 7.4

NP40 buffer with 150 mM NaCl: 1% Nonidet P40
10% Glycerol
50 mM Tris (pH 7.5)
0.1% Sodium Azide
150 mM NaCl

NP40 buffer with 200 mM NaCl: 1% Nonidet P40
10% Glycerol, 50 mM Tris (pH 7.5)
0.1% Sodium Azide
200 mM NaCl

Laemmli-buffer: 200 mM Tris (pH 6.8)
8% SDS
40% Glycerol,
2.4 M β- mercaptoethanol
Bromophenol blue

Antibody	Source	Dilution/ Animal
α-Msk1	Abcam ab82194	1:500 / rabbit
α-NFκB	Abcam ab7970-1	1:1000 / rabbit
α-$MLL1^N$	Millipore 05-764	1:500 / mouse
α-$MLL1^C$	Millipore 05-765	1:500 / mouse
FITC 2^{nd}, α-rabbit IgG	Abcam ab6717	1:1000 / goat
TRITC 2^{nd} ,α-mouse IgG	Dako R0270	1:1000 / goat

Table 2.3: Antibodies used for the Co-IP

3. Results

3.1 Does Msk1 contribute to regulation at MLL1 target genes?

Msk1 (Mitogen- and Stress- activated Protein Kinase 1) is a protein kinase involved in the phosphorylation of H3S10 (Soloaga *et al.*, 2003), but is also downstream of the MAP-kinase signalling pathway (Edmunds and Mahadevan, 2004; Huang *et al.*, 2006). Previous data from the lab (not published) suggest that H3S10p contributes to Hoxa gene activation, for example an enrichment of H3K4me3, H3S10p and Msk1 was observed over the transcriptional start site of Hoxa4 and of Hoxa5 in HPC7 cells. This enrichment was absent in differentiated megakaryoctes, where these active genes are repressed. Furthermore the sites of Msk1 binding correlated with the modifications deposited by proteins of the MLL complex, though the positions of MLL1 and Msk1 deposited marks did not correlate. The data suggested that Msk1 is either part of the MLL complex or acted together with the MLL complex to regulate *Hoxa* gene expression.

3.2 Knock-down of Msk1 in HPC-7 cells

To examine the role of Msk1 on MLL1 target genes, Msk1 should be knocked down. The Nucleofector Kit by Lonza was used to transfect a vector coding for shRNAs in the cells using electroporation. This knock-down was only transient and therefore the optimal time-point for the knock-down, with the lowest Msk1 levels, needed to be identified. Therefore time-courses were performed. For the first trial, samples were taken at 13, 16, 19 and 22 hours after transfection. As shown in Figure 3.1 A, RNA levels were at the lowest level after 13 hours post-transfection, while after 19 hours no difference to the control could be observed. In a second experiment samples were taken at 10, 11, 12, 13 and 14 hours after transfection. It could be shown that the RNA levels at 12 hours were even lower. Under optimal conditions Msk1 RNA transcript levels could be reduced about ~90%.

To reveal that the knock-down, had not only influences on the Msk1 RNA level of the cells, but also on the protein level, transfected cells were collected at 12 hours post-transfection and prepared for immuno-flourescence microscopy. The collected cells were directly centrifuged onto slides and fixed in formaldehyde. After the last sample was collected the cells were stained with α-Msk1 antibody and detected with a 2nd FITC-antibody (Figure 3.1

B). As control HPC-7 cells, transfected with a GFP expression vector, are presented. Msk1 showed a distribution throughout the nucleus, but show a punctate distribution, termed “speckles”. In comparison to this control cells the Msk1-signal in the cells, transfected with Msk1 Knock-down vector, was reduced.

During the transfection the majority of the cells died. In order to enhance the survival of the cells, twice as much SCF (Stem Cell Factor) was added to the HPC7 Growth Medium. As a result clearly more cells survived. However, as a negative effect, the efficency of the knock-down dropped. This was apparent when the effect of the knock-down was examined. The original data sowed a >90% kockdown at transcript level (Fig 3.1 A) but using this „enhanced recovery“ RNA transcript levels were reduced by 50% (Fig 3.2 B).

However, the final question was to examine if the down-regulation of Msk1 has any impact on MLL1 target genes. Therefore a qPCR with primers covering HoxA6 and Meis1 genes was performed. Those target genes were chosen, because they are known target of MLL1. Although the Msk1 knock-down was poor in quality, still a down-regulation of HoxA6 (-27%) and Meis1 (-23%) could be observed (Figure 3.1 B).

Figure 3.1: Knock-down of Msk1 in HPC7 – time course of RNA-levels

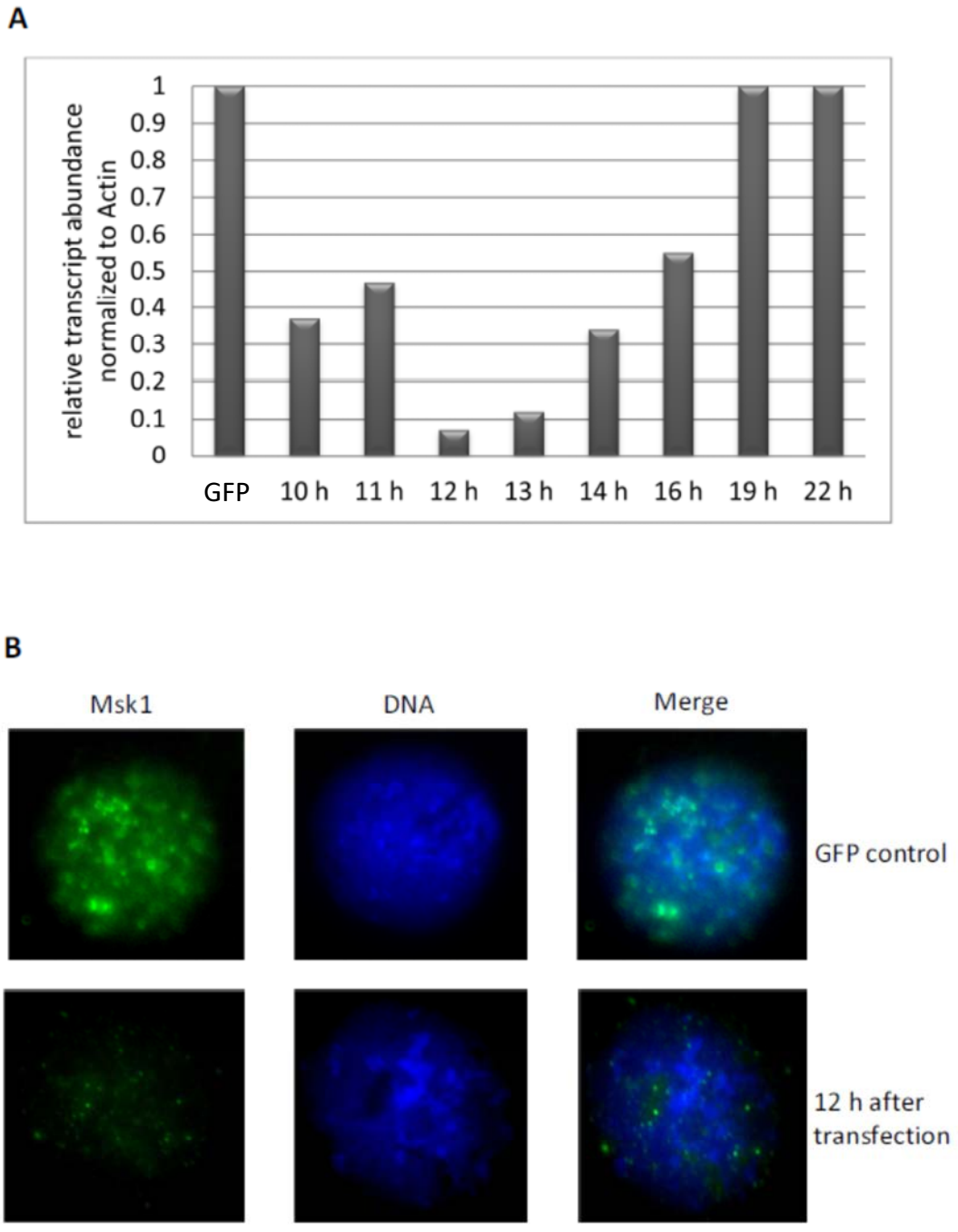

Figure 3.1: Knock-down of Msk1 in HPC7 cells. (A) Cells were transfected and collected at indicated time-points. The qPCR was performed after collecting the last sample. For a positive control cells were transfected with GFP, the RNA levels were normalized to Actin. It could be shown, that after 12 hours the maximum of the knock-down was reached. (B) To confirm the RNA findings, immuno-staining of transfected HPC7 was performed. The reduction of Msk1 could be observed at the protein level, too.

Figure 3.2: Knock-down of Msk1 in HPC7

A

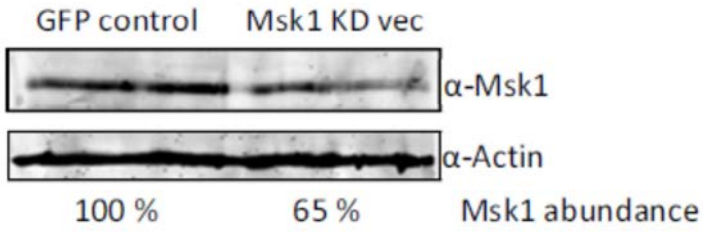

B

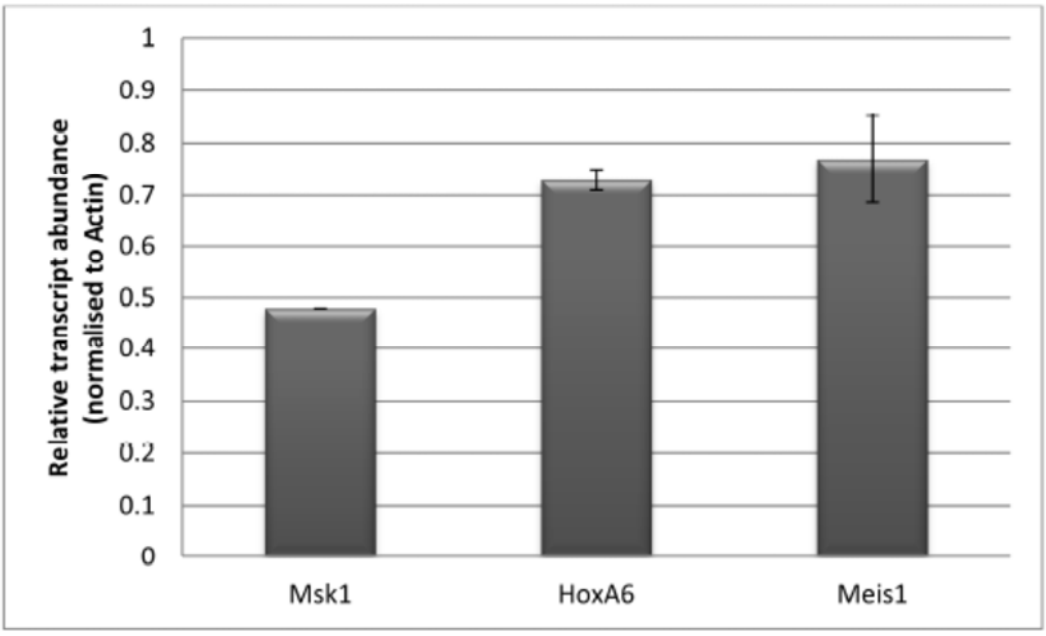

Figure 3.2: Knock-down of Msk1 in HPC7. (A) Cells were transfected with either a GFP control vector or the Msk1 Knock-down vector and collected 12 hours after transfection. A whole cell extract of the samples were prepared and a western blot was performed. The membrane was probed with an antibody against Actin, which showed equal sample loading. The Msk1 antibody a ~35% decreased abundancy of the Msk1 protein. (B) A qPCR was performed 12 hours after transfection. For a positive control cells were transfected with GFP, the RNA levels were normalized to Actin levels. The Knock-down efficency was, with a reduction of only 50% of Msk1 RNA, poor. However, this was enough to show a down regulation of HoxA6 and Meis1 RNA, which are known targets of MLL1, of ~25 %.

3.3 Interaction of MLL1 and Msk1

To adress the question if there is also a physical interaction or if chromatin may „bridge“ interaction (Figure 3.3 A, right panel), Co-Immunoprecipitation in LCL cells was performed. First a pull-down with MLL1 was performed and probed with Msk1. As a positive control a pull-down with NFκB was performed as well, because NFκB is known to interact strongly with Msk1 (Figure 3.3 A, left). Shown are the supernatants (S_1), as well as the beads of the pull downs, that were probed with an antibody against Msk1 (Figure 3.3 B left). In both pull-downs a clear band of the right size of ~90 kDa (indicated by an arrow) could be detected, that was absent in the supernatants. This gives a hint for a interaction of MLL1 and Msk1. Obviously there is a very prominent band of smaller size, that appears as a smear in the NFκB pull-down (indicated by a star), likely to be IgG heavy chain (~55 kDa).

Msk1 and MLL1 are both acting on histone H3. To determine if histone H3 is involved in the interaction of MLL1 and Msk1, the membrane was reprobed with an antibody against the tail of histone H3. As shown in Figure 3.3 B on the left, a signal can be found in all samples, even in the pull-down with NFκB, which is not known to interact with histones. Therefore it needs further investigation and methods to answer the question, if chromatin may bridge the interaction.

To control the findings of the Co-IP, the procedure was reversed (Figure 3.3 B, right). A pull-down with Msk1 was performed and the western probed for MLL1. As MLL1 is very large (full-length 430 kDa), a lower concentrated gel of 10% was run. Because MLL1 consiststs of two fragments (N-terminal ~300 kDa, C-terminal ~180 kDa) the western was probed for these two individual fragments. Unfortunately no MLL1 fragment could be detected, even in the supernatants. This indicates the antibody is unlikely to be adequate for the experiment.

Figure 3.3: Co-IP of MLL1 and Msk1

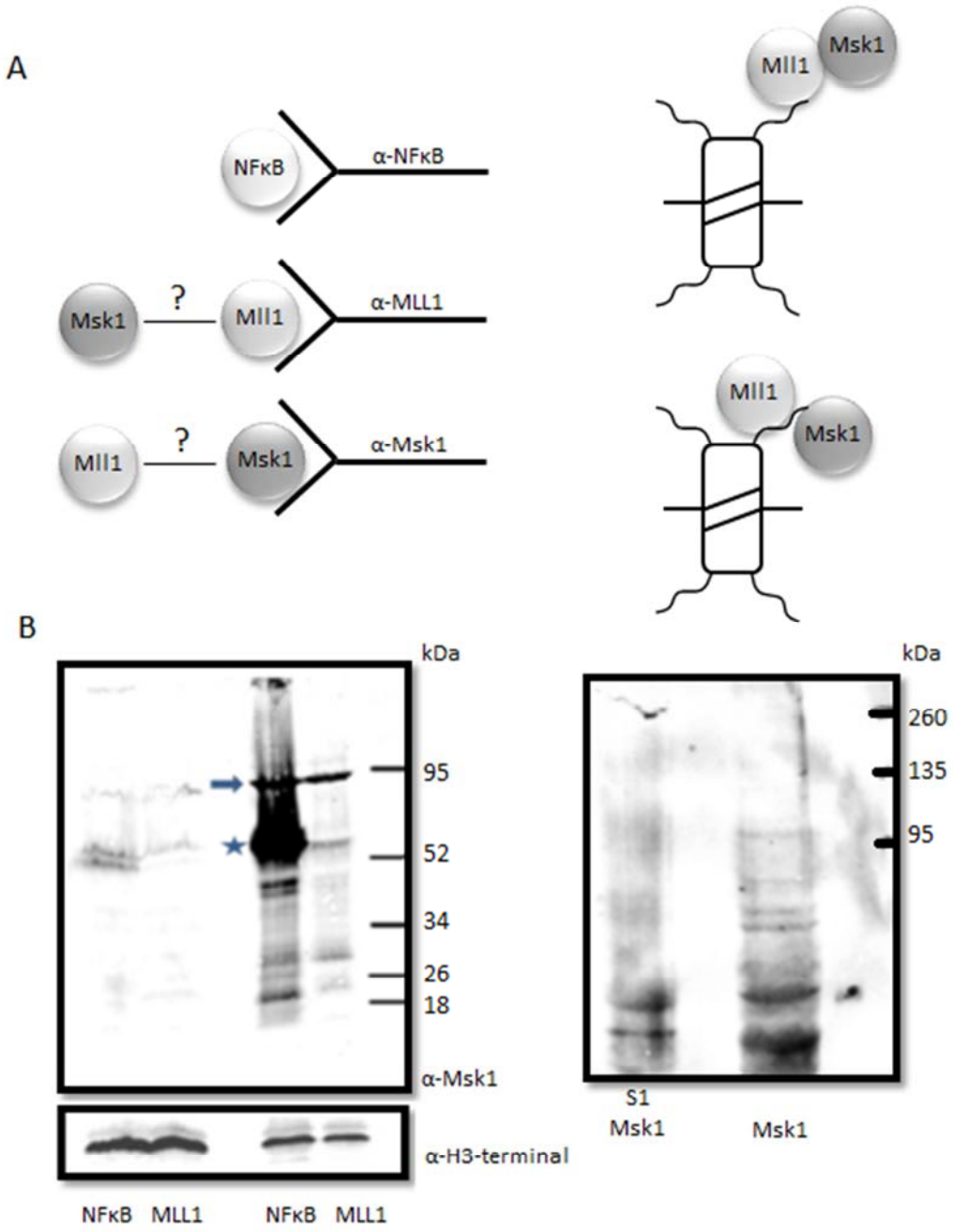

Figure 3.3: Co-IP of MLL1 and Msk1. (A) Representation of the Co-IP experiments. Right panel: It is known that Msk1 and NFkB are binding, so the IP with it was used as a positive control. It should be examined, if MLL1 and Msk1 are interacting and therefore can be pulled down together. Left panel: Two theories are possible. Either MLL1 and Msk1 interact directly with each other (top) or they work on the same site of histone H3 (bottom). (B) Left panel: A Co-IP for MLL1 and NFκB, as a positive binding control, was performed. The supernatant (S1) and the beads were loaded and probed with Msk1 antibody (top) and later reprobed with Histone H3 tail antibody (bottom). Right panel: A Co-IP for Msk1 was performed and the supernatant (S1) and the beads were loaded. The membrane was probed with antibodies against the N- and the C-terminal of MLL1.

3.4 Immunofluorescence microscopy of Msk1 and MLL1

To see if in the cell Msk1 and MLL1 are in close proximity, a localisation study on either LCL cells or HPC7 cells was performed. The cells were centrifuged on slides and stained with an antibody against Msk1, which was detected by a 2ndFITC-conjugated anti rabbit IgG antibody, and with an antibody against MLL 1, which was detected by a 2ndTRITC-conjugated anti mouse IgG antibody. In both cell types Msk1 and MLL1 showed the same distribution, whereas Msk1 tended to form „speckles“ and MLL1 not. However, the staining was not equal in all cells. On some cells an overall staining could be observed, on others it was more punctate and on others there was a disconnection of Msk1 and MLL1. The latter was especially observed on cells in which the mitotic chromosomes were visible. This lead to the hypothesis, that the localisation of the proteins differ during the cell cycle.

To examine if these differences in staining are cell cycle dependent the cells were either treated with Thymidine or Colcemid. Both substances arrest the cells in the cell cycle at specific time points (Figure 3.4 A). Thymidine blocks the cell during the S-phase, so that as a result the cell population is enriched with cells in G1/S-phase. Colcemid inhibits the formation of the mitotic spindle, which leads to a cell population with cells in G2-phase or mitosis. To control the effect of Thymidine and Colcemid a flow-cytometric analysis was performed (Figure 3.4 B).Propidium Iodide staining was used as a measure of nuclear DNA content (i.e. n-number). In the left diagram a unsyncronised cell population was measured and a typical cell cycle diagram with two peaks (one for G0/G1 and one for G2/M) were obtained. In the middle diagram a Thymidine treated population was analysed. As expected only the first peak (G0/G1) was obtained. In the right diagram a population treated with Colcemid was examined and the second peak (G2/M) was observed. However the block was not perfect and as G0/G1-phase shoulder demonstrated.

The further colocalisation study was then repeated with one of the two different subfraction of arrested cells (Figure 3.5 A-D). In A and C an equal, all-over staining of the cells with both, Msk1 and MLL1 antibody, dominated. In B and D cells, which were in mitosis, were shown. In those cells Msk1 and MLL1 seemed to disconnect from the DNA (stained with DAPI) and tend to form more „speckles“ (B) or to be packed in structures outside the nucleus (D).

Figure 3.4: Cells arrested in the cell cycle

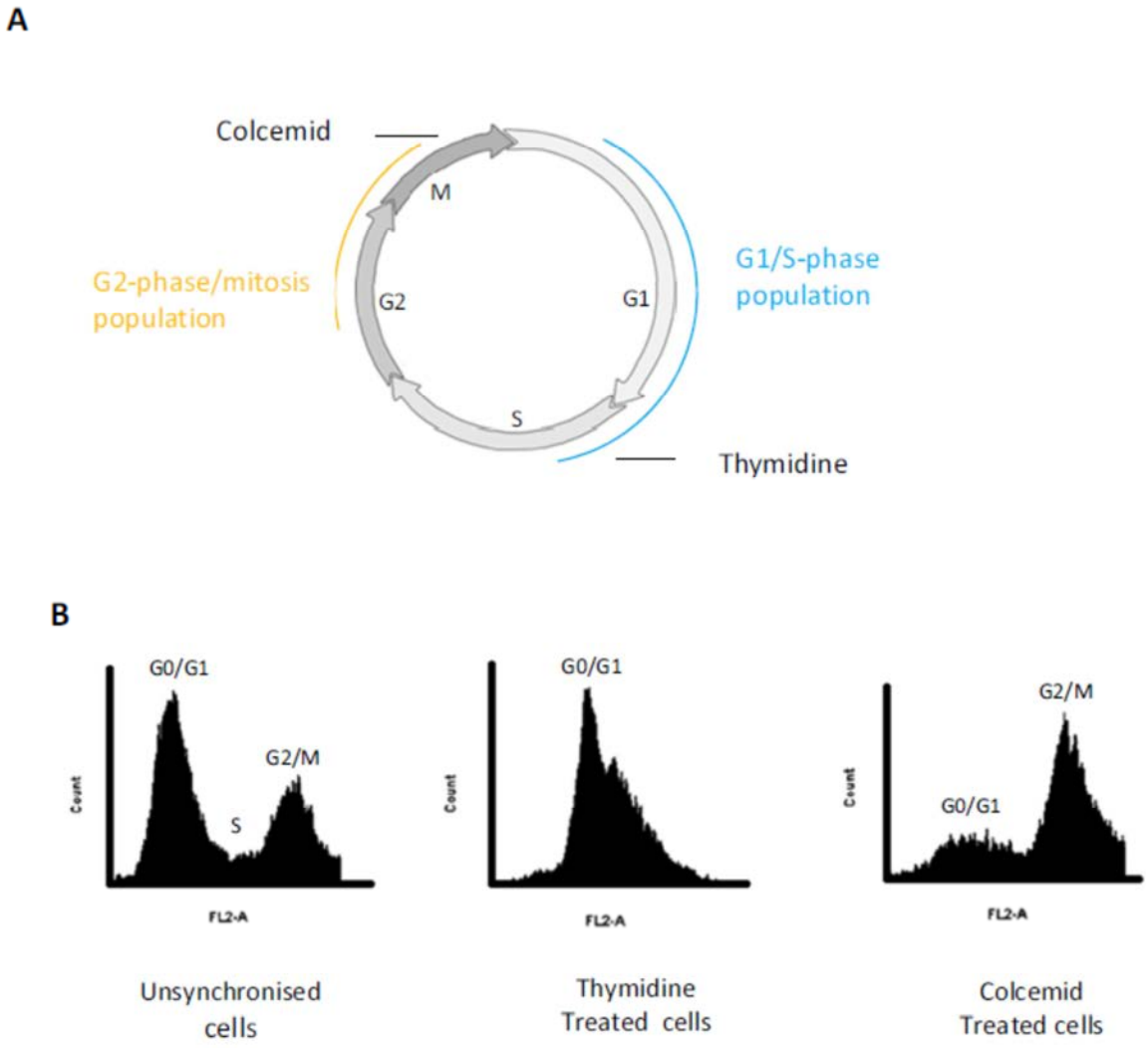

Figure 3.4: Cells arrested in the cell cycle. (A) In order to examine the behaviour of Msk1 during the cell cycle, LCL cells were either treated with Colcemid, which inhibits the cells in mitosis, or with thymidine, which inhibits the cells in the S-Phase. (B) To control the effects of Colcemid and Thymidin a Flow cytromety analysis was performed, using propididum iodide incorp to assess nuclear content (n number).

Figure 3.5: MLL 1 and Msk1 Immuno-Staining

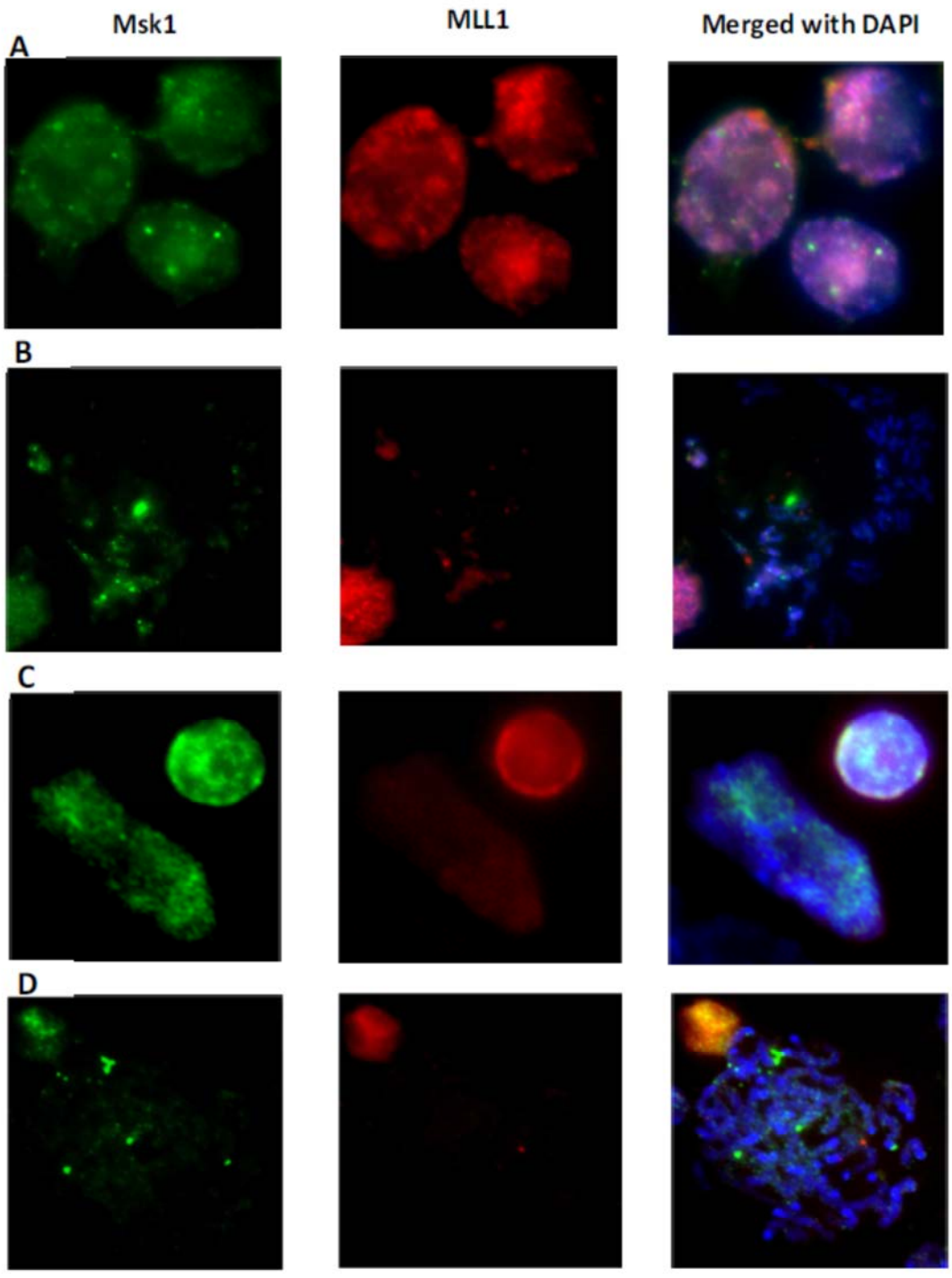

Figure 3.5: MLL1 and Msk1 Immuno-Staining

(A) LCL cells treated with Thymidine
(B) LCL cells treated with Colcemid
(C) HPC7 cells treated with Thymidine
(D) HPC7 cells treated with Colcemid.

Green=Msk1, Red=MLL1, Blue=DAPI

3.5 Msk1 during the cell cycle

The observation, that apparently in some parts of the cell cycle less protein is (i. e. Fig 3.5 BD) and that Msk1 and MLL1 are distributed differently throughout the cell cycle lead to the question if the total amount of these proteins differed, too. To answer this question equal volumes of LCL cells were either treated with Thymidine or Colcemid to obtain G2/Mitosis and G1/S population. For comparison the same volume of untreated LCL cells were taken. After incubation whole cell lysis extracts were prepared and then 200 µl of cell extract were loaded on a gel. A Western Blot was performed and the membrane was first incubated with an antibody against Msk1 and for a loading control with an antibody against Actin. A representative Western Blot is shown in Figure 3.6 A. As the actin control revealed there was more Actin present in the untreated cell population, than in the treated ones, with the lowest Actin levels seen in the Colcemid treated cell population. However an enrichment of Msk1 in the Thymidine treated cell population could be observed.

The experiment was repeated twice and the results are shown in figure 3.6 B. Depending on the total abundancy of protein and quality of the antibodies, the Actin signal was much stronger than the Msk1 signals. As indicated in the blot (Figure 3.6 B, upper panel), the loading differed between the different experiments. By normalising for this loading artefact, differences in the strength of the Msk1 signals could be observed (Figure 3.6 B, lower panel). Taking this and the observation of the Actin loading control into consideration, it can be said, that in the unsyncronised population as well as in the Colcemid treated one the abundancy of Msk1 is more or less the same. A small enrichment in the Thymidin treated population could be observed. Taken together it can be determined, that although the Msk1 distribution changes in the different cell cycle stages, the total amount of protein is roughly the same, with maybe a slight enrichment in G1/S-phase.

Figure 3.6: Msk1 abundance during the cell cycle

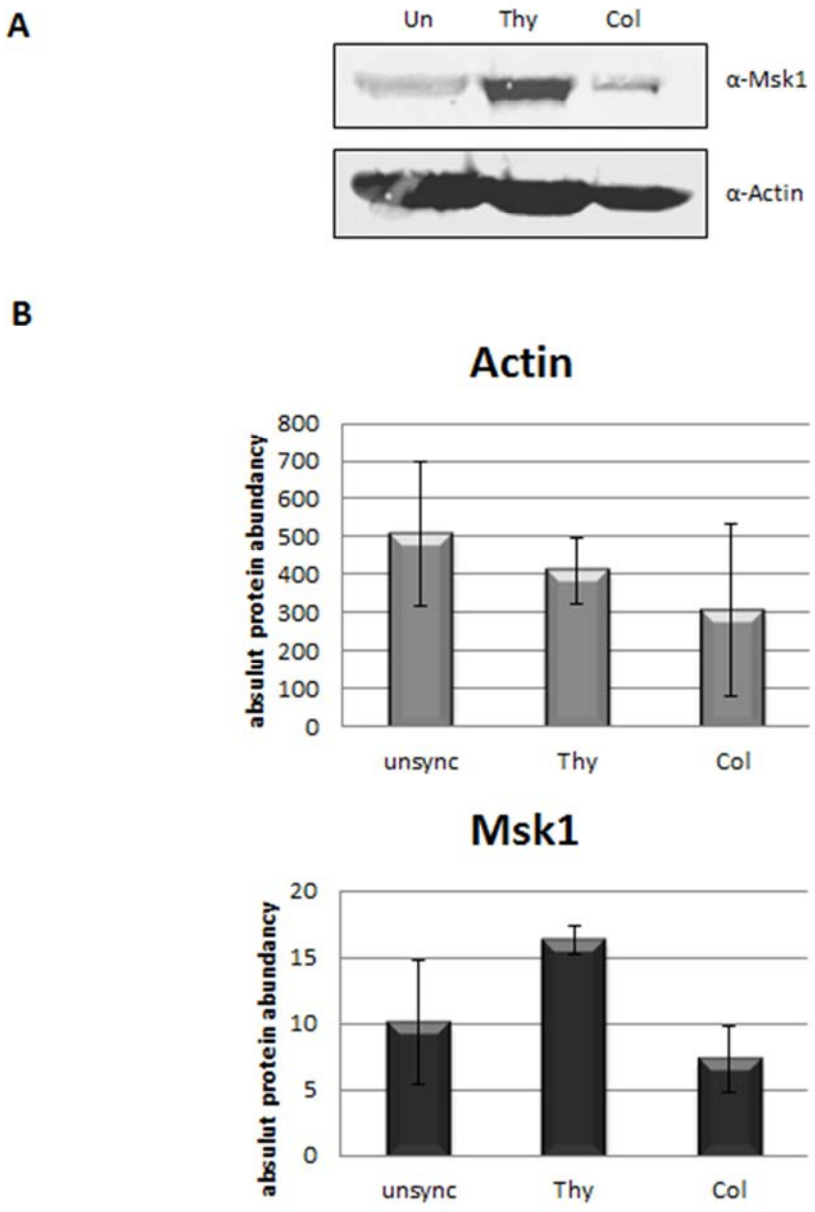

Figure 3.6: Msk1 during the cell cycle. (A) Western Blot. LCL cells were treated with either Thymidine or Colcimid to arrest them during the cell cycle. As a control unsynchronised cells are shown as well. First the membrane was incubated with α-Msk1 Antibody and to control the loading then with β-Actin antibody. (B) Quantification. Three individual experiments were performed. Signals were quantified using arbitary units.

4. Discussion

MLL1 is the human homologue of Drosophila's trithorax (TRX), a group of transcriptional regulators that positively maintain expression of homeobox (HOX) transcription factor genes, which play an important role in the expansion of the progenitor cells of the myeloid line in haematopoesis (Milne 2002, Slany 2005). However less is known about how MLL is regulated. Results from the lab (data not published) suggested that Msk1 (mitogen- and stress-activated protein kinase 1) may play a part in it. Msk1 is phosphorylated and activated by the mitogen-activated proteinkinase (MAPK) pathways and was identified as a H3 kinase (Dyson 2005). The MAPK pathways regulate eukaryotic gene expression in response to extracellular stimuli (Edmunds 2004). In the lab (data not published) it could also been shown, that H3S10p contributes to Hoxa gene activation, for example an enrichment of H3K4me3, H3S10p and Msk1 was observed over the TSS of Hoxa4 and of Hoxa5 in undifferentiated HPC7 cells. This enrichment was absent when these genes are active in differentiated megakaryocytes, where the genes are repressed. Here I have examined if Msk1 takes part in the regulation of MLL1 target genes and how it might be involved with the MLL1 complex.

4.1 Does Msk1 take part in the regulation of MLL1?

To examine the role of Msk1 in the regulation of MLL1 a knock-down of this protein in HPC7 cells was established. Under good conditions a decrease of 90% of the RNA could be generated, after 12 hours of incubation, which resulted in a strong Msk1 protein decrease. However, the harvest was poor, as the majority of the cells died. In order to enhance the survival of cells, twice the amount of SCF was added to the recovery media, with the result, that more cells survived but the knock-down efficiency dropped. Under normal conditions those cells were probably seriously damaged instead of transfected and would have died. As the samples of the transfected cells were so precious, further experiments were carried out with the material, which was less efficiently transfected. qPCR revealed that only ~50% RNA transcript reduction could be obtained under these conditions. Nevertheless it led to a decrease of the total amount of Msk1 protein of ~35%. It could be demonstrated that this was enough to down-regulate the RNA appearance of two known MLL1 target genes, HoxA6

and Meis1, down nearly a quarter. This is a strong indication for the regulatory involvement of Msk1 on MLL1 target genes. Still, there are questions to answer. It is not yet shown, that the down-regulation of Msk1 also significantly effects the level of HoxA6 and Meis1 proteins, are the acting components in a cell. It also has to be proved, if the regulation of MLL1 target genes by Msk1 is a general effect on MLL1 target genes and if yes, what it means for the fate of the cells.

It also should be examined if a physical interaction between those two proteins exists (Figure 4.1). Therefore Co-Immunoprecipitation were performed. When a pull down with MLL1 was carried out and probed with an antibody against Msk1 a signal of 90 kDa could be detected. This argues for a interaction of Msk1 and MLL1. In the reverse experiment, however, this interaction could not be demonstrated. This is probably due to the experimental procedure, this was an initial trial and maybe with other antibodies and/or refined procedure the interaction can be demonstrated, too. First of all the MLL 1 antibodies need to be tested for immuno-detection on a membrane. So far the antibodies have been established and used for immuno-staining. Second, MLL1 is a very big protein, which needs to be run on a lower percentage SDS-gel and longer in blotting. Third and finally, it seems that protein degradation is a problem and this may reduce detection. Using Co-IP, the hypothesis, that Msk1 and MLL1 interact via chromatin and/or histone H3, which therefore acts as a “bridge” (Figure 4.1), should be tested. Unfortunately histone H3 could be detected in all samples and in the control pull-down with NFκB, which does not interact with histone H3, so no statement can be made. This is probably due to the procedure, as histones are known to bind non-specifically to beads.

Figure 4.1: Hypothesis of the Regulation of MLL1 by Msk1

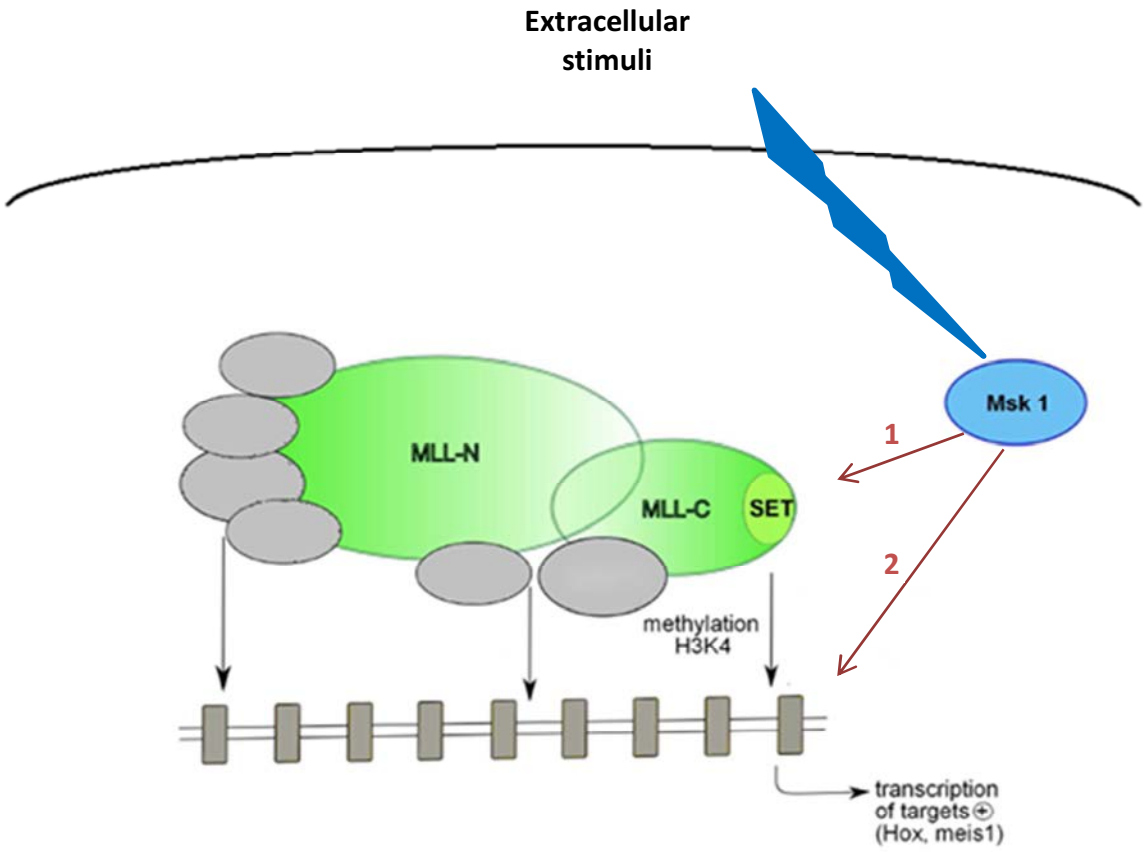

Figure 4.1: Hypothesis of the Regulation of MLL1 by Msk1. There are indications, which suggest that MLL1 is regulated by Msk1. So far two model hypothesis are plausible. First (1) Msk1 and MLL1 directly interact with each other or second (2) Msk1 and MLL1 interact indirectly via chromatin.

4.2 How is Msk1 involved with the MLL1 complex?

To investigate how Msk1 and MLL1 interact with each other, a co-localisation study was carried out. Cells were fixed on slides and stained with antibodies for Msk1 and MLL1. Msk1 and MLL1 showed nucleus specific, over all staining. As both proteins act on chromatin, this was not a surprise. But as they showed no specific pattern it is impossible to say if they are co-localised or if they just happened to be at similar locations as they are acting on similar/same sites. Although no statement about the co-localisation could be made, it attracted attention, that the staining was not similar in all cells. Most cells were stained throughout the nucleus, but some cells showed a speckled, punctated staining, especially for Msk1 and on some cells the staining seemed to be separated from the chromatin. The latter was mostly the case when also the mitotic chromosomes were visible. This led to the hypothesis, that the distribution of Msk1 and MLL1 varied during the cell cycle. To test this theory cells should be blocked (i.e. with thymidine) and released to synchronise the cell population through the cell cycle and samples of every stage of the cell cycle could then be taken. It was found that the cells could be trapped in the G1 phase, but after the thymidine was washed out the cells refused to procced further through the cell cycle. The same could was observed when the cells were serum-starved and accumulated in G1 phase.

To examine cell-cycle phase dependency, two subpopulations were created by arresting cells with thymidine (G1/S phase) and with colcemid (G2/Mitosis). Although the arrest generated by these agents was not perfect (i.e. in the G2/Mitosis population a lot of G0/G1 phase cells were detected), an enrichment could be well observed. In the G1/S phase population the majority of cells showed an all-over nuclear staining. During mitosis, which was easy to identify because of it metaphase chromosomes, Msk1 and MLL1 was evicted from the chromatin and were stored in speckles or vacuoles. Nevertheless in the G2/mitosis population the other cells were either stained over all or speckley, but it was not possible to say in which stage of the cell cycle they were exactly.

Having observed, that the connection of Msk1 and MLL1 differs in the two populations the question arose if the total content of protein differed. To answer this question whole cell lysis extracts were prepared and a western blot performed or the two populations. A slight enrichment of Msk1 in the G1/S phase population could be observed, but this was preliminary data, where the loading control β-actin was varying a lot and measurements between the three experiments varied a lot, too. One problem obviously was that the same

volume of cell culture was prepared for treatment with thymidine and colcemid as well as taken for control. However no cells were counted, which may have resulted in different amounts of cells in the different experiments. Thymidine and Colcemid may have cell toxic effects and decreased the numbers in the treated cell populations. When repeating this experiment it should be ensured, that the same numbers of cells are taken when preparing whole cell extracts. The other thing to think about is, if actin is a good loading control or if its content may vary in the cell cycle naturally too. To rule possible fluctuations of the loading control out, it would be better to use histone H3 as a loading control. The amount of histone H3 is stable through the cell cycle and the C-terminal antibody is not subject to by any modifications, which would lead to artefacts.

The biggest disadvantage is, that the division into those two populations only mimics cell cycle distribution. As it was not possible to synchronise and release the cells again, the other option is to sort cell by FACS. This would yield distinct sets of cells and a discrimination between the cells in G1-, S- and G2-phase would be possible

4.3 Concluding remark

In this study, it could be demonstrated that Msk1 does have a regulatory effect on MLL1. However the methods need to be refined as discussed above and further investigation are needed to determine how, or whether Msk and MLL complex interact, what the general consequence of the regulation is, and if Msk1 could be used as target for leukaemia treatment.

It was also demonstrated that Msk1 and MLL1 both seem to follow a cell-cycle dependent distribution, and it can be speculated that the total amount of protein may vary slightly. Further investigations need to be done to make these data conclusive and to address the questions if this has an impact on how MLL-deposited marks during the cell cycle are retained.

Taken together, a link between two cellular key processes could be provided. Epigenetic gene activation by MLL1 was connected to the response to extracellular stimuli by Msk1 as a down-stream target of the MAPK pathway. This is consistent with the described role of Msk1 as a remodeller of chromatin on immediate early genes by histone H3 phosphorylation (Drobic, Perez-Cadahia et al. 2010). The findings of the project suggest that Msk1 may act on multiple MLL1 target sites. The finding that Msk1 acts on trithorax

mediated processes via MLL1 is backed-up by the finding that Msk1 mediates epigenetic changes during embryonic stem cell differentiation (Lee, McCool et al. 2006) and that Msk1 is able to reverse polycomb complex induced silencing (Gehani, Agrawal-Singh et al. 2010; Lau and Cheung 2011). Resulting from the fact, that there are several human MLL methyl-transferases and two Msk isoforms with different distinct function it would be interesting to examine if there is a whole new complex network of interactions.

Part II

Project 2

„The molecular basis of inhibitory signalling during neuronal regeneration“

This project is submitted in partial fulfilment of the requirements
for the award of the MRes

Abstract

Limited neuronal regeneration following CNS injury is due to interactions between the myelin derived inhibitors and the Nogo-receptor (NgR) ternary complex, consisting of NgR, p75 and Lingo1. The inhibitory role of Lingo-1 presents a novel target for nerve repair and remyelination therapies. Lingo1 is one member of a large group of CNS enriched membrane proteins, with a LRR and an Ig domain in their ectodomain. Recently, other members of the LRR-Ig protein family, namely Amigo-proteins, have been reported in the context of neuronal development, survival and regeneration. This study has combined biochemical, binding and structural approaches to further characterise the function of Amigo proteins, with a particular emphasis on whether Amigo proteins can substitute for Lingo1 in forming a ternary NgR complex. The ectodomains of Amigo1 and Amigo3 were expressed and successfully purified by Ni-NTA affinity and gel filtration chromatography. Based on BIAcore binding analyses, whereas Amigo 1 and Amigo 3 demonstrated no binding with p75, weak interactions were found with NgR. In addition, initial cross-linking experiments with BS^3 indicated, that Amigo1, but not Amigo 3, can self-associate forming dimers in solution. Finally, crystallisation trials for Amigo1 ectodomain identified a condition that yielded suitable sized crystals for preliminary X-ray diffraction experiments.

1. Introduction

1.1 The central nervous system

The mammalian central nervous system (CNS) consists of more than 20 billion neurons, which are connected by trillions of synapses. The formation of synapses, called synaptogenesis, is a complex process, including axon path-finding, target recognition and the elaboration of the synaptic contact. To ensure that functional neuronal circuits are specifically installed, guidance mechanisms have evolved to regulate the growth and connection of neurons in the developing brain (Benson, Colman et al. 2001). Synaptogenesis is a process that is not limited to the development of the CNS, as the CNS requires constant refinement, with modification and elimination of old synapses and generation of new ones in response to aging, learning and damage (Yiu and He 2006). CNS injury can disrupt this process leading to neuronal death, axon degeneration and demyelination. Following a CNS injury a glial scar is formed within days around the injury site and forming a physical barrier for axonal sprouting. Furthermore, scar-associated molecules function as chemical inhibitors that block axon regeneration generating an additional barrier for axon regeneration (Giger, Hollis et al. 2010). Damage of CNS myelin further attenuates axonal growth through the action of myelin derived degradation products. These have been characterised in the last decade and include Nogo, myelin-associated glycoprotein (MAG) and oligodendrocyte-myelin glycoprotein (OMgp), all of which bind to the Nogo Receptor (NgR) (Yamashita, Fujitani et al. 2005). The NgR receptor is a trans-membrane protein with multiple Leucine-rich repeats (LRRs) in its ectodomain (He, Bazan et al. 2003).

1.2 LRR domains and the LRR superfamily

The LRR domain is important for facilitating protein-protein interactions and is found in bacteria, fungi, plant and animals. The LRR motif is generally rich in hydrophobic residues, preferentially leucines and are generally 20-29 residues long containing a characteristic conserved 11 residue sequence motif (LxxLxLxxNxL where x=amino acid, L=leucine and N=asparagine (Kobe and Kajava 2001). Other hydrophobic residues (phenylalanine, Isoleucine or valine) can substitute for the leucine and asparagine residues. Proteins with LRR architecture usually form curved solenoid structures, in which each turn consists of one repeat, with hydrophobic residues packed into the inner core of the solenoid providing protein stability. In addition, the LRRs are usually flanked by caps, which protect the hydrophobic residues of the first and the last LRR module (Bella, Hindle et al. 2008).

The LRR motif is highly conserved and present in a variety of proteins with diverse functions ranging from innate immunity regulation through Toll-like receptors (Schuster and Nelson 2000) to neural development, neurite outgrowth and synapse formation (de Wit, Hong et al. 2010). Proteins with LRR motifs often possess other characteristic modules such as Ig and fibronectin domains and the large LRR superfamily can therefore be divided into subgroups based on their architecture, including the LRR (LRR domain only), LRR-Ig (LRR + Ig domain) and the LRR-Toll (LRR + Toll/Interleukin-1 receptor domain) groups (Kobe and Kajava 2001).

1.3 The Nogo-Receptor Complex

During the search for binding partners of Nogo, a glycosylphosphatidylinositol (GPI) linked protein with multiple LRRs in its ectodomain was identified as a receptor that mediates inhibitory signals to axonal outgrowth. This newly identified protein was termed the Nogo Receptor (NgR) and binding of Nogo led to collapse of axonal growth cones (Fournier, GrandPre et al. 2001). The ligand binding domain of the NgR is comprised of nine LRRs, which are flanked by two cysteine-rich capping modules, that form a solenoid structure (He, Bazan et al. 2003). The NgR shows the typical LRR motif sequence (xLxxLxxLxLxxNxLxxLPxxFx), in which the leucine is often replaced by phenylalanine. The concave surface of the NgR is enriched in aromatic residues, which form two patches that are separated by a group of charged residues that shape the ligand binding site. A second more discrete binding site is located at the C-terminal end of the ectodomain, formed by LRRs at the C-terminal end and the bulkier C-terminal flanking cap and offers a recognition

site for accessory signalling receptors, which are necessary for signal transduction since NgR as a GPI linked protein cannot signal independently (He, Bazan et al. 2003). NgR has been shown to bind to two co-receptors, namely $p75^{NTR}$ and Lingo-1 and together they form a functional ternary complex (Figure 1.1) (Mi, Lee et al. 2004).

$p75^{NTR}$ is a type I transmembrane protein and member of the neutrophin family of growth factors which mediates intracellular signalling by activating the RhoA-pathway (Wang, Kim et al. 2002). Rho molecules are membrane linked GTPases, which activities are controlled internally by Guanine nucleotide exchange factors and are involved in cytoskeletal organization (Schmidt and Hall 2002). Interestingly, $p75^{NTR}$ is highly expressed in the developing nervous system but decreases during the postnatal period and adulthood. In the adult brain only a subpopulation of mature neurons express $p75^{NTR}$. Previous studies have highlighted that TROY, a member of the TNF receptor family, can substitute for $p75^{NTR}$ function (Park, Yiu et al. 2005).

The second co-receptor, Lingo-1, is exclusively expressed in the CNS. The ectodomain of Lingo-1 is made up of two distinct modules a LRR and an Immunoglobulin (Ig)-like domain. The Lingo family contains three variants (Lingos 2-4), which are highly conserved (44% - 61% amino acid sequence identity between the Lingo paralogues and 99% sequence identity between mouse and human orthologues) (Mi, Sandrock et al. 2008).

Collectively, the components of the NgR Complex provide ligand binding (via NgR), facilitate signalling (via $p75^{NTR}$) and promote stability (via Lingo-1). Since Lingo-1 is restricted to neural tissues and has a critical role in transmitting inhibitory signals within the CNS via the NgR complex, it represents an attractive candidate for therapeutic targeting to improve recovery following CNS injury.

Figure 1.1: The Nogo-receptor complex

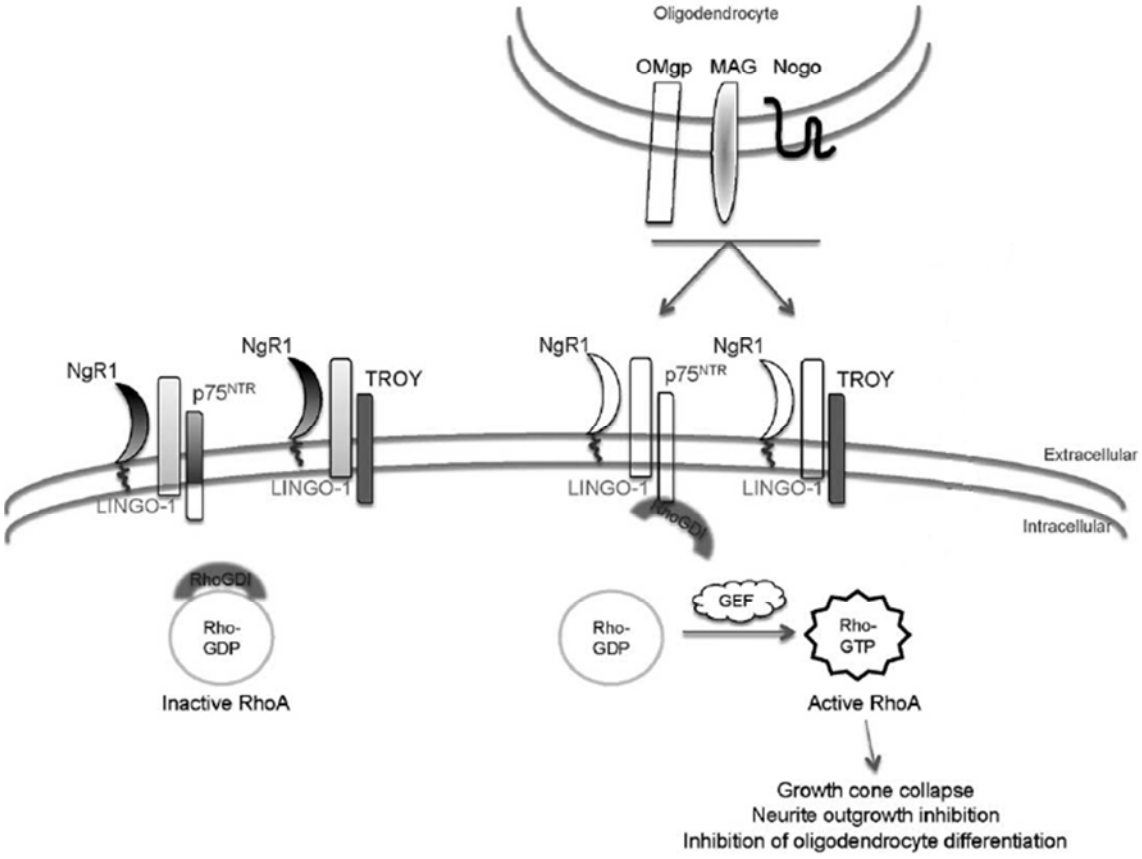

Figure 1.1: The Nogo-receptor complex. The Nogo-receptor complex consists of the NgR, p75NTR and Lingo-1. Troy can substitute for p75NTR function by forming a ternary complex with Lingo-1 and NgR (left side). Ligands of the NgR complex include the myelin derived proteins OMgp, MAG and Nogo. Their binding activates the NgR complex, which binds to the Rho guanine dissociation inhibitor (RhoGDI). This leads to the activation of Rho-GDP by guanine nucleotide exchange factor (GEF) and into the collapse of the growth cones in axons and the inhibition of neuronal outgrowth. **(McDonald, Bandtlow, Reindl, 2011)**

1.4 Lingo-1

Lingo-1 is a type I transmembrane protein with an ectodomain composed of 12 LRR, which are folded in the typical solenoid structure and flanked by N- and C-terminal caps. It is closely followed by an Ig-domain, which related in nearly a 90^{o} angle to the last LRR. The Ig module is connected to the transmembrane and cytoplasmic tail regions by a stalk (Figure 1.2 A). Lingo-1 forms a ring like tetramer structure that leads to clustering of charged patches on the inner and outer rims of the ring (Figure 1.2 B), which may facilitate the binding of multimeric signalling complexes on the cell surface. This is in accordance with the putative role of Lingo-1 as an adapter for co-receptors. Although the Ig domain does not facilitate tetramer formation, it suggests it plays a role in co-receptor recognition (Mosyak, Wood et al. 2006).

Expression analyses of the NgR components NgR1, $p75^{NTR}$ and Lingo-1 revealed only a small time-frame for parallel expression, occurring during the late postnatal stages. (Mi, Miller et al. 2005). Furthermore, Lingo-1 is expressed in several brain regions lacking NgR1 or $p75^{NTR}$ expression, which indicates that Lingo-1 may participate in signalling events that are independent of the NgR complex (Llorens, Gil et al. 2008). Additional functions may include effects on neuronal survival via down-regulation of EGFR (Mi, Sandrock et al. 2008) and regulation of oligodendrocyte differentiation and myelination via NGF by interacting with the Lingo-1/TrkA receptor complex (Figure 1.2 C) (Lee, Yang et al. 2007). Also, Lingo-1 has been determined to be a negative regulator of oligodendrocyte differentiation and myelination, as the loss of Lingo-1 function increases branching and myelination (Mi, Miller et al. 2005, Zhao, Jin et al. 2007). It remains to be seen whether other members of the LRR-Ig family have analogous functions to Lingo-1.

Figure 1.2: Structure and Function of Lingo1

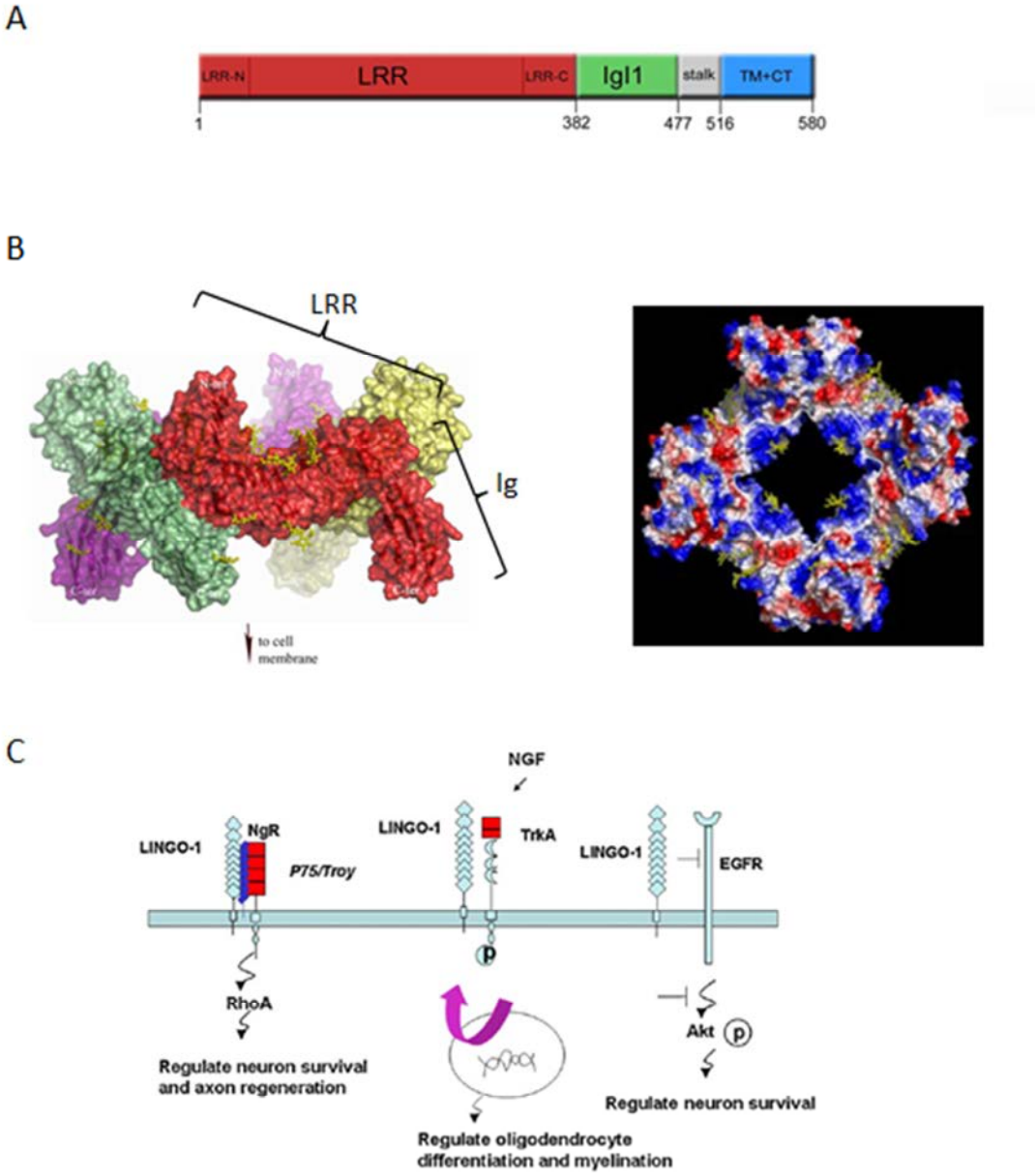

Figure 1.2: Structure and function of Lingo-1. (A) Schematic domain structure of Lingo-1 showing the N-terminal LRR-domain (red), the C-terminal Ig domain (green), the stalk region (grey) and the transmembrane/cytoplasmic domain (blue). (B) Four Lingo-1 molecules form a ring like structure (left side, LRR and Ig domain are indicated). Electrostatic surface potential for Lingo-1 tetramer highlights the highly positive charged surface surrounding the inner ring structure (right side, view of the top surface; blue=positive and red=negative charge). (C) Lingo-1 participates in several signalling pathways. It is member of the NgR complex controlling axon regeneration (left) and is activated by the NGF/TrkA receptor complex to control oligodendrocyte differentiation and myelination (middle). Lingo-1 also interacts with EGFR and influences the Akt signalling pathway (right) **(Mosyak et al. 2006 and Mi, Sandrock, Miller 2008).**

1.5 The LRRIg family and the Amigos

The LRRIg family has multiple related genes with a common structure consisting of a variable frequency of LRRs, which are typically flanked by an N-and C-terminal caps, closely followed by a single Ig-domain (Figure 1.3). The LRRIg family also includes the Amigo-proteins, which share approximately 12-30 % sequence identity with the Lingo family (Figure 1.4) (Kobe and Kajava 2001; Chen, Aulia et al. 2006)

The Amigos were discovered in a screen for effectors of amphoterin, a heparin-binding protein that promotes neurite outgrowth and is enriched in the growth cones of neural cells. One transcript was predominantly up-regulated and therefore called amphoterin-induced gene and ORF (Amigo). Based on sequence homology two related proteins (Amigo 2 and Amigo 3) were identified. The Amigos are type I transmembrane proteins, with a signal sequence for secretion and a transmembrane sequence. The extracellular region of all Amigos encompasses six LRRs, a cysteine rich N- and C-terminal cap as well as an Ig domain (Kuja-Panula, Kiiltomaki et al. 2003). It is a highly conserved protein; mouse and rat exhibit 95% sequence homology whereas mouse and human show 89 % sequence identity. Also, Amigos 1, 2 and 3 share ~50% sequence identity. Additionally the Amigo proteins show about 12 – 30 % sequence homology to Lingo1 although they have six LRRs less than Lingo1 (Figure 1.4). Notably, the expression patterns of Amigos show a great variation. Amigo1 is primarily expressed in nervous tissue, whereas Amigo2 is mainly found in the cerebellum, retina, liver and lungs. In contrast, expression levels for Amigo 3 are more widespread (Kuja-Panula, Kiiltomaki et al. 2003).

In a second independent study the Amigo family was discovered in a different context. Amigo2 was discovered as a protein that was involved in depolarization and NMDA-dependent survival of cerebellar granule neurons and was named Alvin. Overexpression of Alvin led to inhibition of KCl induced apoptosis (Ono, Sekino-Suzuki et al. 2003).

At present, very little is known about the function of Amigo family members, particularly in relation to axon regeneration and myelination.

Figure 1.3: Members of the LRR-Ig family

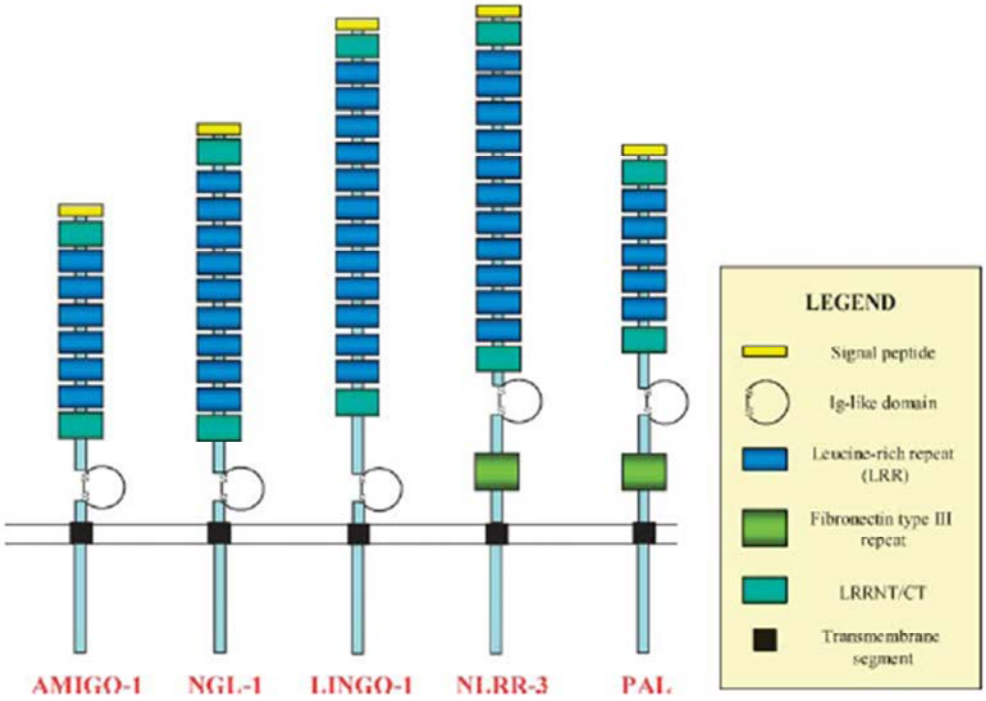

Figure 1.3: Members of the LRR-Ig family. Members possess tandem LRR domains followed by an Ig module within their ectodomains. Note that NLRR-3 and PAL contain an additional fibronectin type III repeat **(Mi, Aulia, Li, Tang 2006).**

Figure 1.4: Sequence comparison of Lingo1 and the members of the Amigo family

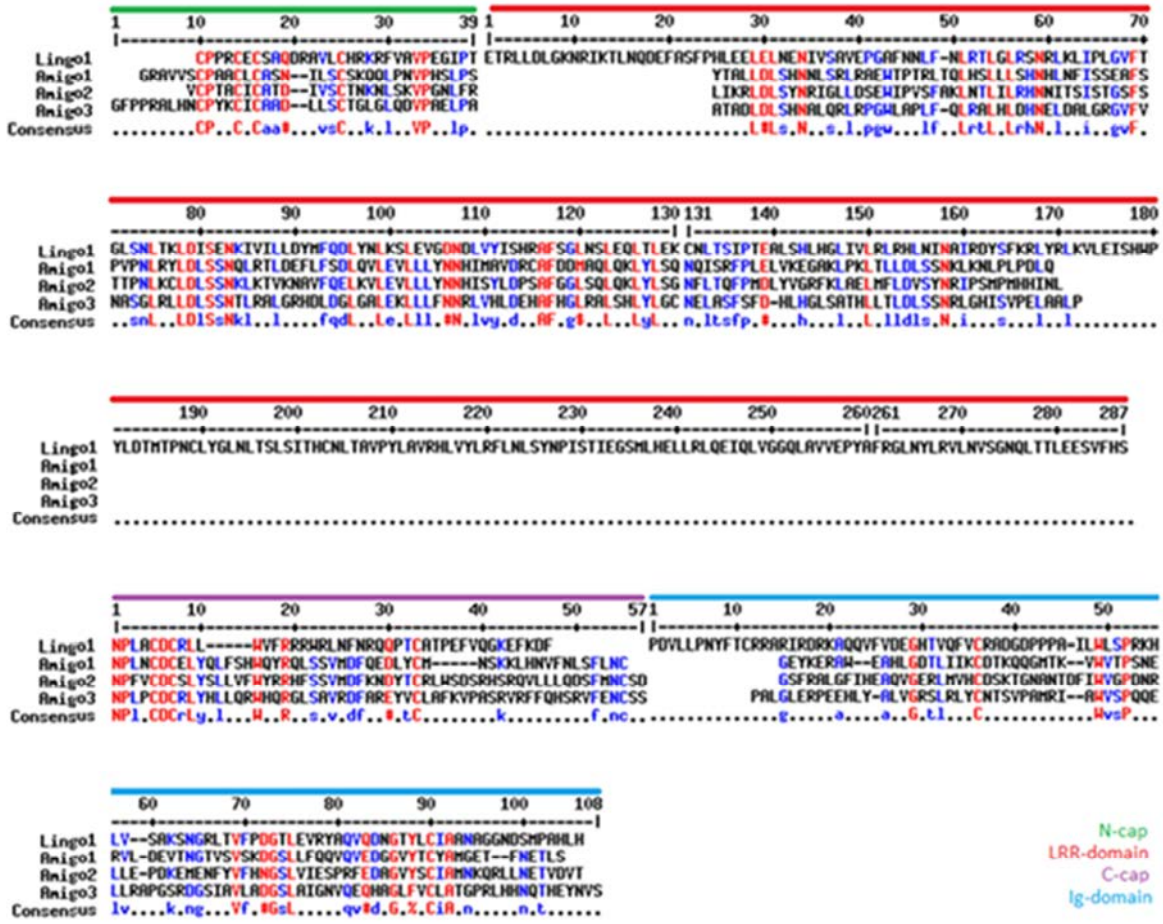

Figure 1.4: Sequence comparison of Lingo1 and the members of the Amigo family. (shown are human protein sequences). The Amigo proteins show the same protein architecture like Lingo1. Their ectodomains contain a LRR domain, which is flanked by a N- and a C-terminal cap, as well as a Ig domain. The biggest difference is that Lingo1 contains 12 Leucine rich repeats, while the Amigo proteins contain only 6. Nevertheless 12 % of their sequences are highly conserved (red letters) and another 20 % are modestly conserved (blue letters).

1.6 Therapeutic relevance of the LRRIg family

One of the key features following a CNS injury is that limited recovery is often observed. This is due to the physical and molecular factors of the glial scar in conjunction with the growth inhibitory environment. In this context proteins, which are responsible for the inhibition of nerve outgrowth, are potential therapeutic targets. Lingo-1 is a particularly attractive candidate because of its restricted expression in the CNS (McDonald, Bandtlow et al. 2011). More recently, soluble Lingo-1-Fc (ectodomain of Lingo-1 coupled to Fc region, serves as an antagonist for the NgR complex signalling pathway by competing with endogenous Lingo-1) was used in a rodent spinal cord injury model demonstrating promotion of axonal sprouting and increased oligodendrocyte and neuronal survival (Ji, Li et al. 2006). Lingo-1 may also play a significant role in Parkinson's disease as its expression levels are elevated in the substantia nigra of patients with this disease. In a rodent model of Parkinson's disease, the administration of Lingo-1-Fc led to enhanced neurite outgrowth and showed neuro-protective effects (Inoue, Lin et al. 2007).

Therapy with anti-Lingo-1 antibodies that antagonize the effect of endogenous Lingo-1 have also been of interest. As Lingo-1 modulates the differentiation of oligodendrocyte precursor cells (OPC), one possibility is that anti-Lingo-1 antibodies could promote OPC differentiation and myelination and therefore offer a potentially novel strategy for the treatment of multiple sclerosis (MS) (Mi, Miller et al. 2009).

Despite these findings it still remains unknown whether Lingo-1 is the most functionally relevant member of the LRR-Ig family as a component of the Nogo-receptor complex and therefore a critical player in the inhibition of neuronal differentiation.

1.7 Aims

Recent Microarray experiments comparing injured CNS tissue to non-injured CNS tissue, showed up-regulation of Amigo proteins, whereas Lingo-1 levels remained unchanged after injury. This suggests, that the Amigo proteins (particularly Amigo3) could be functionally relevant in CNS regeneration. In addition, subsequent co-immunoprecipitation experiments found that the Amigo proteins could be co-purified with NgR and $p75^{NTR}$, suggesting that the Amigo-proteins may substitute for Lingo-1 in forming a ternary NgR complex (Lab M. Douglas, unpublished data). For Lingo-1 a direct binding of its ectodomain to NgR and p75 could be demonstrated (Mosyak, Wood et al. 2006). It is possible that Amigo proteins could

bind to the NgR and p75 similar to Lingo1, forming a more efficient Nogo-receptor-complex for activation. In order to formally test this hypothesis soluble His-tagged ectodomains of the Amigo family (Amigos 1 - 3) will be over-expressed using insect cell expression systems and purified with Ni-NTA and size exclusion chromatography. Purified soluble Amigo ectodomains will be utilised for biochemical and biophysical analyses including cross-linking experiments, BIAcore protein-protein binding analysis and structural studies. Collectively, these experiments will go towards gaining a greater understanding of the role of Amigos in forming NgR complexes and in verifying whether Amigos are suitable therapeutic targets following CNS injury.

2. Materials and Methods

2.1 Cell culture

2.1.1 Cultivation of S2 cells

Protein expression vectors encoding the proteins of interest were co-transfected into the Drosophila cell line S2 alongside a separate vector conferring Hygromycin B resistance. The cells were grown in a selecting medium consisting of "complete growth medium" supplemented with 0.03% Hygromycin B. Cells were transferred into fresh medium, containing 10% conditioned medium, every 5 days. Small volumes of culture (15-20 ml) were seeded at a density of $1x10^6$cells/ml into T-75 flasks and incubated at 27^{o}C in a non-humidified incubator, allowing the cells to grow semi-adherently. Larger volumes (>125 ml) were seeded at a density of $1.2x10^6$cells/ml and grown in 500ml Erlenmeyer flasks , with 0.05% Pluronic F-68 surfactant (Gibco) to prevent clumping of the cells. The flasks were incubated at 27^{o}C at constant shaking rate of 80rpm. Once cells reached a density of 3.5-$5x10^6$cells/ml, protein expression was induced by adding $CuSO_4$ to a final concentration of 500µM. After five days the cell supernatant was collected by centrifugation (two spins; first at 50 rpm for 10 minutes and second at 2500 rpm for 10 minutes). The supernatant was collected and following the addition of 0.02% of Sodium-Azide, stored at 4^{o}C.

Complete growth medium:	Schneiders Drosophila medium + Glutamine (Biological Industries) 10% FCS (PAA the cell culture company)

2.2 Protein Methods

2.2.1 Protein Dialysis

S2 supernatant was placed into dialysis tubing (cut-off size 12 kDa, Sigma) and dialysed against PBS buffer (1:10 ratio) overnight at 4^{o}C.

PBS: 2.7 mM KCl
137 mM NaCl
8.1 mM Na_2HPO_4
1.76 mM KH_2PO_4, pH 7.4

2.2.2 Nickel affinity chromatography

1ml of Nickel-beads (Ni-NTA agarose stored in 20% ethanol, Qiagen, binding capacity of 25mg/ml) was added to an Econo column (BIO-RAD). The ethanol was drained off and the beads were washed with 10 ml of 1xPBS + 10 mM Imidazole. The dialysed S2 supernatant was flown over the beads by gravity at 4^{o}C overnight with a slow flow-rate. On the next day, the column was washed with 1xPBS + 10 mM Imidazole to remove non-specific proteins. For elution of His-tagged proteins, the column was filled with 1xPBS + 250 mM Imidazole (~10 ml) and left for 30 minutes. After the incubation period the eluted proteins were collected in 1ml fractions and quantified by spectrophotometry using UV absorbance (280nm; see below).

2.2.3 Protein Concentration and buffer exchange

For protein concentration Centrifugal Filter units (Millipore) were used, with a molecular weight cut off of 10 kDa. The small units (0.5 ml capacity) were centrifuged at 6500 rpm for 10 minutes at 4^{o}C. The large units (15 ml capacity) were centrifuged at 2100 rpm for 20 min at 4^{o}C. These units were also used for buffer exchange steps, whereby the protein was concentrated to a small volume and the units were filled up with the desired buffer and centrifuged again. This step was repeated at least three-times to ensure complete buffer exchange.

2.2.4 Quantification of Protein concentration

Protein concentrations were determined by measuring absorbance at OD_{280nm} using a Biophotometer (Eppendorf). The absorbance at OD_{280nm} is a linear function of the molar concentration: $Abs_{280} = \varepsilon \times c \times l$, whereas ε is the extinction coefficient (L mol^{-1} cm^{-1}), c the protein concentration (g/l) and l the path length of the sample (mostly l=1cm). If ε is known the protein concentration can be calculated from the Abs_{280} measurement. The absorbance of a protein sample at 280 nm is due to Tryptophan (W), Tyrosine (Y) and disulfide bonds (SB) within the protein and therefore the ε value of a protein can be calculated by using the following formula: $\varepsilon = n_W \times 5500 + n_Y \times 1490 + n_{SB} \times 125$. Notably if the disulfide bonding is unknown $n_{SB} = 0$ (Mach, Middaugh, Lewis, 1992).

2.2.5 Size exclusion chromatography

Protein purification by size exclusion chromatography was performed using a Pharmacia FPLC system. For smaller amounts of protein sample (~1 mg) the HR200 column was used, whereas for larger amounts (>1 mg) the S200 column was used. Prior to loading protein samples, size exclusion columns were equilibrated with the desired buffer (mostly Tris-buffer). During the gel filtration purification run defined fractions were collected by a fraction collector (integrated part of the FPLC system). Elution profiles were generated by measuring OD_{280} of the flow-through. Inspection of the elution profile allowed the identification of peak fractions, which were analysed by SDS-PAGE to confirm purity of protein samples.

Tris-buffer:	50 mM NaCl 20 mM Tris, pH 8.5

2.2.6 Trichloroacetic acid (TCA) protein precipitation

To 1 volume of 100 % (w/v) TCA stock 4 volumes of protein sample were added and the sample incubated for 10 minutes on ice. The mixture was centrifuged at 14000 rpm for 5 minutes. The supernatant was removed, without disrupting the protein pellet, which was washed twice with 200 µl ice-cold acetone and centrifuged at 14000 rpm for 5 minutes. The pellet was dried at 95 ^{o}C for 10 minutes.

2.2.7 Sodium dodecyl sulphate polyacrylamide gel electrophoresis (SDS-PAGE)

Proteins were separated according to size (Laemmli, 1970). For the detection of the Amigo-fusion proteins (Amigo1-LRR 28 kDa, Amigo1-LRRIg 38 kDa, Amigo3-LRR 28 kDa, Amigo3-LRRIg 38 kDa) a 15% SDS separating gel was prepared. Normally 10 µg of protein samples or TCA precipitated protein pellets were resuspended in SDS Loading buffer containing DTT and incubated at 95°C for 10 minutes (reducing conditions = R) or resuspended in Loading buffer containing no DTT and not boiled (non-reducing conditions = NR) before loading onto the gel. A voltage was applied across the gel (constant 100 V for the stacking gel and 150 V for the separating gel), for one hour allowing proteins to differentially migrate based on their size. Following electrophoresis the gel was stained with Coomassie brilliant blue for 30 minutes and destained overnight with destain buffer.

15% SDS gel: 5ml Bis-acrylamide (30%Acrylamide-0.8% Bis)
375 µl Tris-HCl, pH 8.8
100 µl 10% SDS
100 µl 10% Ammonium Persulfate
4 µl TEMED made up to 10 ml with distilled water

Stacking gel: 670 µl Bis-acrylamide (30% Acrylamide-0.8% Bis)
125 µl Tris-HCl, pH 6.8
100 µl 10% SDS
40 µl 10% Ammonium Persulfate
4 µl TEMED made up to 10 ml with distilled water

SDS reservoir buffer: 50 mM Tris
0.384 M glycine
0.1% SDS

Reducing 5xSDS loading buffer: 40 mMTris, pH 6.8
0.75 % (w/v) SDS
8 mM DTT

Non-reducing 5xSDS loading buffer: 40 mM Tris, pH 6.8
0.75 % (w/V) SDS

Destain buffer: 20% Methanol
10% Acetic Acid

2.2.8 Immuno-detection of proteins on nitrocellulose membranes ("Western Blot")

Protein samples were first separated by SDS-PAGE as described above. The separated proteins were transferred (Towbin et al., 1979) onto a PVDF membrane (Hybond LFP, GE Healthcare) for one hour (300V/400mA) using transfer buffer. The efficiency of transfer was checked by staining the membrane with Ponceau Red. The membrane was incubated for one hour or overnight at 4°C in Blocking Buffer in order to minimize non-specific antibody binding. Afterwards the membrane was washed three times with 1xTBS + 0.1 % Tween-20 for five minutes. The membrane was incubated with the primary antibody diluted in 1xTBS + 0.1% Tween + 3% BSA for 1 hour at room temperature. The membrane was washed three times, each for 5 minutes, with 1xTBS + 0.1 % Tween-20. The secondary antibody (HRP-conjugated, anti-mouse,) was added in 5% milk + 1xTBS + 0.1% Tween. Binding was visualised by using the "EZ-CCL Chemiluminescence Detection Kit for HRP" (Biological Industries). Briefly, this involved mixing 500 µl of solution A with 500 µl solution B and then incubating for five minutes at room-temperature. The mixture was added onto the membrane and incubated for five minutes at room-temperature. The membrane was placed into a cassette and taken to the dark-room, where a light sensitive filter (Amersham Hyperfilm^{TM} MP, GE Healthcare) was placed for 10 or 20 seconds on the membrane before the filter was developed.

Transfer buffer:	25 mM Tris 192 mM glycine 20% methanol
Blocking Buffer:	5% dried milk powder 1 x TBS 0.1% Tween-20

Antibody	Source	Dilution/Animal
α-Histidine (C-terminal)	Invitrogen	1:5000/mouse
2nd HRP, α-mouse IgG	Sigma	1:33333/goat

Table 2.1: Antibodies used for western blot

2.3 Functional Studies

2.3.1 Small-scale crystallization trials

Initial crystallization trials were screened using the "hanging drop vapour diffusion" method with the nano-litre Mosquito crystallisation robot (TTP LabTech). To identify the optimal conditions for crystal formation three commercial screens (each containing 96 unique conditions) were used (Table 2.2). Briefly, 100 µl of crystallization condition was added into each well of a 96 well IWAKI plate. The Mosquitorobot was used to pipette nano-litre drops (100 nl protein-solution + 100 nl crystallization buffer) onto a 96-well plate seal (TTP LabTech). The plate seal was then inverted on to the IWAKI plate such that the appropriate drops were placed over their corresponding crystallization buffers. The crystallisation plates were incubated at 24°C. After one week the plates were analysed for crystals using a light microscope. Conditions that yielded small crystals or needles were selected and optimised. For all conditions that provided crystals, negative controls with protein substituted for buffer were set up.

Screen	Company
JCSG+	Molecular Dimension
Wizard I + II	Emerald Bio Systems
Index	Hampton Research

Table 2.2: Commercial Screens used for crystallization trials

2.3.2 Large-scale crystallization trials

The scale up was performed according to the "hanging drop vapour diffusion method". In a 24 well Linbro plate the edges of the wells were coated with vacuum grease and 1 ml of crystallization buffer was added to each well. On a coverslip 1 µl of crystallization buffer was mixed with 1 µl of protein solution. The coverslip was inverted on to the well and pushed down so that an air-tight seal was obtained. The plate was incubated for several days at 24^{o}C before checking for crystals by light microscopy.

2.3.3 BIAcore binding analysis

For the BIAcore protein binding analysis the BIAcore system 3000 with auto-sampler, the BIAcore 3000 control software and a CM5 Sensor Chip (GE Healthcare) with four flow-cells (FC) were used. A new chip was docked into the system and buffer primed using water and normalized with BIAnormalization buffer (GE Healthcare). Following this the buffer was changed to the running buffer (HBS-PE). Then the Fc Antibody Rz108ea was amine coupled to the surface of all four chambers. Firstly the surface was activated with the EDC/NHS mix (10 µl/min for 7min). Secondly the Fc-Antibody ligand was passed over the surface (10 µl/min for 7min). The surface was saturated with Ethanolamine-HCl (10 µl/min for 7min) and finally washed with NaOH (10 µl/min for 7min) and Gly-HCl (10 µl/min for 7min) to strip off all non-covalently associated proteins. All four flow chambers were washed with buffer at a flow rate of 5µl/min. In the next step recombinant proteins were immobilized. The recombinant proteins (NgR-Fc, p75-Fc) were diluted 1:2 in the HBS-EP running buffer and injected over appropriate flow-cells (FC 1=no proteins, FC 2=NgR-Fc, FC 3=p75-Fc, FC 4=NgR-Fc and p75-Fc). After the flow-cell surfaces were prepared the purified protein sample was injected and the binding response recorded.

Solutions for amine coupleing:	5 mM NaOH 0.1 mM Gly-HCl, pH 2.5 1 M Ethanolamine α-Fc antibody in 10 mM Na-acetate, pH 4.5 EDC/NHS 1:1 mix (Ethyl-3carbodimide hydrochloride/N-Hydroxysuccinimide mix)

Antibodies/recombinant proteins	source	concentrations
α-Fc antibody	Antibody production facility, University of Birmingham	25 µg/ml
NgR-Fc, recombinant human	R&D systems	100 µg/ml
p75-Fc, recombinant human	R&D systems	100 µg/ml

Table 2.3: Antibody and recombinant proteins used for BIAcore analysis

2.3.4 Cross –linking analysis

For the Cross-linking of proteins three Cross-linkers with spacer-arms of different length were used according to the manufacturers instructions. The cross-linkers were dissolved in 20 mM Hepes buffer, pH 8.5 and the proteins were diluted in the same buffer. 5-10 µg of protein were incubated with 50-fold molar excess of cross-linkers at room-temperature for 30-60 minutes. The reaction was quenched by the addition of 1 µl of 1 M Tris, pH 8.5.

Cross-linker	Source	Spacer-arm length
Dimethyl pimelimidate (DMP)	Mike Douglas	9.2 Å
BS^3	Pierce	11.4 Å
Sulfo-EGS	Pierce	16 Å

Table 3.4: Reagents used for cross-linking experiments

2.3.5 Deglycosylation of proteins

The deglycosylation kit (PNGase F, New England BioLabs) was used according to the manufacturers instructions. 5-10 µg of protein were diluted with deanaturation buffer and heated for 10 minutes at 100 ^{o}C. Then the reaction buffer was added to the denatured protein, as well as the deglycosylation enzyme. The mixture was incubated at 37^{o}C for one hour.

3. Results

3.1 Can Amigo-proteins substitute for Lingo1 in forming a ternary NgR complex?

Following CNS injury, myelin derived inhibitors of axonal regeneration bind to the NgR/p75/Lingo1 ternary complex on neurons (Yiu and He 2006). Since Lingo1 is partially responsible for the inhibition of nerve outgrowth and has an expression pattern, which is restricted to the CNS, therapeutic strategies to block its function are a potential route promoting CNS recovery following injury (McDonald, Bandtlow et al. 2011). However, Lingo1 is only one member of the LRRIg protein family, a set of receptors which share the same protein architecture (Ji, Li et al. 2006). Other members of this family, specifically Amigo family members, have been shown to be up-regulated following injury to CNS tissue (Douglas, M. Personal communication). Furthermore it was possible to co-immunoprecipitate Amigo1 or Amigo3 with p75 and the NgR (Douglas, M. Personal communication). These data suggest that Amigo proteins may substitute for Lingo1 in forming a ternary complex with p75 and NgR and therefore play a key inhibitory role in response to CNS injury.

3.2 Experimental Approach to study the Amigo proteins

Previous studies on Lingo1 have highlighted that the functionally important domains include the extracellular LRR and Ig domains. As Lingo and Amigo family members share the same overall LRR-Ig fold, the Amigo ectodomains were similarly cloned and fused to a His-tag sequence to facilitate subsequent purification (Figure 3.1 A).

At the beginning of the project two constructs were cloned and transfected into cells, namely Amigo1 LRR and Amigo 1 LRRIg. Cloning of Amigo3 LRRIg was completed mid-way through the project. (Figure 3.1 B).

Figure 3.1: Expression and purification of the Amigo proteins

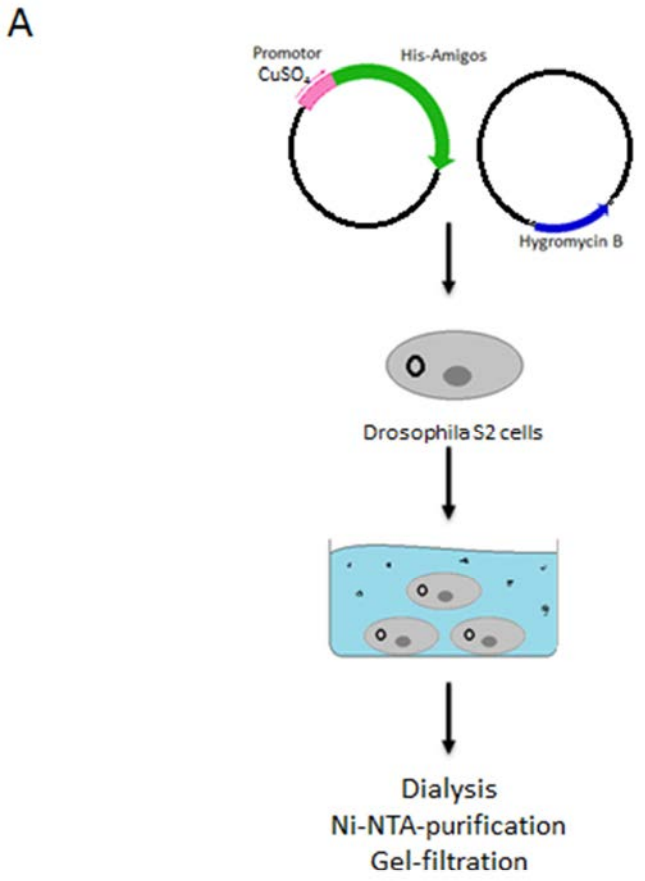

Figure 3.1: Overall expression and purification protocol for the Amigos. (A) Expression vectors, encoding either for the His-tagged Amigo-protein or Hygromycin B resistance, were cloned and co-transfected into Drosophila S2 cells (carried out by Protein Expression Facility, University of Birmingham). The stably transfected cells were kept in culture and bulked up. After the induction of Amigo protein expression with CuSO4, the Amigo proteins were secreted into the supernatant. The supernatant could be harvested by centrifugation after five days. The supernatant was dialysed against PBS buffer and the Amigo proteins purified by Ni-NTA affinity. To further improve the purity gel filtration chromatography was performed. (B) During this project three Amigo constructs were cloned for functional and structural studies. For Amigo1 the whole ectodomain containing both the LRR and the Ig domain was cloned, as well as the ectodomain lacking the Ig domain. For Amigo3 the whole ectodomain with the LRR and the Ig domain was cloned.

3.3 Purification of Amigo Proteins

3.3.1 Purification of Amigo1 LRR

To analyse protein expression, 20 µl of supernatant of the Amigo1 LRR culture were taken and a western blot was performed using an anti-His antibody, as no characterised anti Amigo antibodies are currently available. Robust expression in the supernatant was shown (Figure 3.2 A left). Initially, a small volume of supernatant (250 ml) was tested for purification. The supernatant was dialysed against PBS and then purified by Ni-NTA chromatography, with a yield of 438 µg (1.1 mg out of 1 l). In order to get first hints on purity and the native structure of Amigo1 LRR, reduced (R) and non-reduced (NR) samples were analysed by SDS-PAGE. No differences between the reduced and non-reduced samples could be observed and although an enrichment of the protein could be observed (arrow) the purity was only moderate, with contaminating proteins still visible. (Figure 3.2 A right). To improve purity, the next batch of supernatant (250 ml), was proccesed with an additional gel-filtration step using a HR200 column (yield after Ni-purification 345 µg, 1.4 mg out of 1l). The elution profile (Figure 3.2 B left) yielded three peak fractions all of which were analysed by SDS-PAGE to determine which peak corresponded to Amigo1 LRR. The third peak fraction contained the Amigo1-LRR protein (arrow), but the purity was still low (Figure 3.2 B right). To further increase purity, the Ni-NTA purification protocol was modified by increasing the concentration of Imidazole in the wash buffer (from 10 to 20 mM) for the last batch of supernatant (500 ml). Although, the elution profile of the HR200 column now showed only two peaks, there was a considerable reduction in protein yield (Figure 3.2 C left). When analysing the peak fractions by SDS-PAGE (Figure 3.2 C middle) it was demonstrated that the second peak contained Amigo1 LRR in high purity. To confirm the identity of the purified protein a western blot was performed using the His antibody (Figure 3.2 C right). In conclusion, although pure Amigo1 LRR could be obtained, the final yield was poor. In each case after purification, there were only sufficient levels of protein for TCA precipitation and analysis by SDS-PAGE.

Figure 3.2: Expression analysis and Purification of Amigo-1 LRR

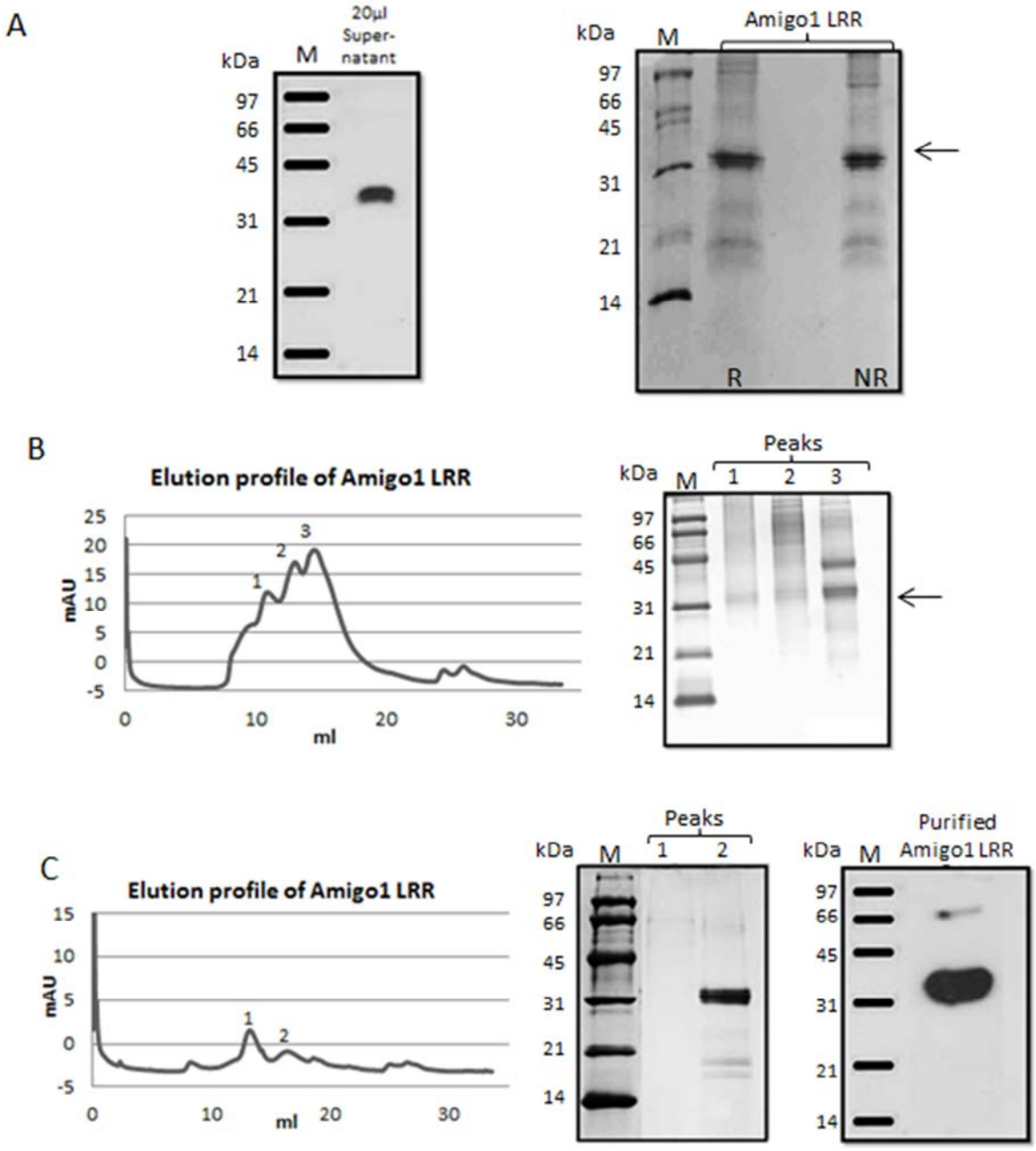

Figure 3.2: Expression analysis and purification of Amigo-1 LRR. (A) Test expression and Ni-NTA purification of Amigo1 LRR. Western blot analysis of 20 µl of supernatant (left). SDS-PAGE analysis of fractions following purification by Ni-NTA chromatography (right). (B) Optimization of purification. An additional gel-filtration step was included to the purification protocol. Elution profile of HR200 column (left). Peak fractions analysed by SDS-PAGE (right). (C) Further Optimization of purification. The Ni-beads were washed with 20 mM Imidazole in the wash buffer during the Ni-NTA purification step. Elution profile for Amigo1 LRR with the HR200 gel filtration column (left). Peak fractions analysed by SDS-PAGE (middle). The identity of the purified protein was confirmed by western blot (right).

3.3.2 Purification of Amigo1 LRRIg

As previously, Amigo1 LRRIg expression was analysed by western blot using 20 µl of supernatant revealing strong expression levels (Figure 3.3 A left). For a small-scale purification 250ml of supernatant was dialysed against PBS buffer and purified by Ni-NTA and gel filtration (HR200) chromatography (Figure 3.3 A middle). SDS-PAGE analysis revealed that the protein was pure even prior to the gel-filtration purification step. No differences between the reducing and the non-reducing conditions could be observed (Figure 3.3 A right). One striking observation was that on SDS-PAGE gel Amigo1 LRRIg migrated at a higher molecular weight (~45 kDa) than the expected calculated molecular weight based on its primary sequence (~38kDa). It was suggested that the protein was glycosylated. More remarkably, the protein also eluted much earlier from the column than expected for its size. Figure 3.3 B shows the elution profiles of Amigo1 LRRIg and MHC class I overlaid following purification by gel filtration (using the S200 column). Although the MHC complex (45 kDa, marked by asterisk) is theoretically larger than Amigo1 LRRIg (38 kDa), it elutes later (Figure 3.3 B). This potentially suggested that the protein forms a dimer in solution. Finally, a large-scale purification (750 ml supernatant) was purified as described above, this time using the S200 gel filtration column. The elution profile provided a single peak and the peak fraction analysed by SDS-PAGE demonstrated sufficient levels of purity for subsequent studies (Figure 3.3C left and middle). The identity of the purified Amigo LRRIg was confirmed by western-blot analysis using His-antibodies (Figure 3.3 C right). From one litre of supernatant it was possible to purify ~5 mg of protein after Ni-NTA purification and ~2.5 mg after gel-filtration.

Figure 3.3: Expression analysis and Purification of Amigo1 LRRIg

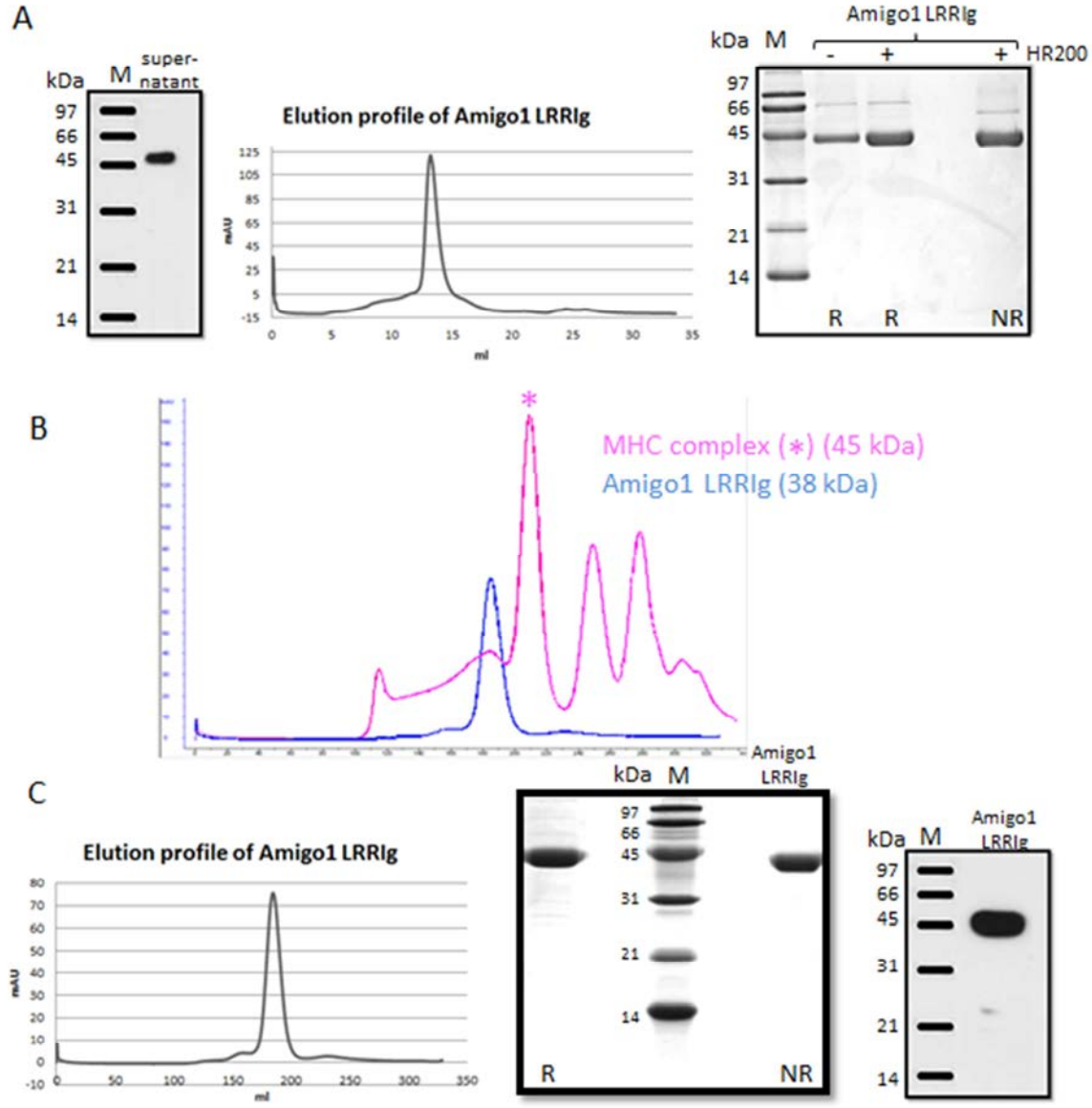

Figure 3.3: Expression and purification of Amigo1 LRRIg. (A) Test expression and purification. Western blot analysis of 20 µl S2 cells supernatant (left). Small-scale purification of Amigo1 LRRIg. 250 ml of S2 cell supernatant was dialysed and purified over Ni-beads and gel-filtration column (elution profile of HR200 column; middle). Analysis of peak fractions by SDS-PAGE following purification by Ni-NTA and gel filtration chromatography (right). (B) Overlaid elution profiles of MHC complex (pink) and Amigo1 LRRIg (blue) following runs on the HR200 gel-filtration column. Amigo1 eluted unexpected early form the column. (C) Large-scale purification. 750 ml of S2 cell supernatant were purified by Ni-NTA and gel filtration (elution profile of S200 column left side). Analysis of peak fractions by SDS-PAGE following purification with gel filtration (middle). Western blot analysis of purified Amigo1 LRRIg (right).

3.3.3 Purification of Amigo3 LRRIg

The expression of Amigo3 LRRIg was tested on 20 µl of S2 cell supernatant by western blot analysis using His-antibodies. Although a Ponceau-Red staining indicated that sufficient sample was loaded, no signal could be detected, indicating low expression of Amigo3 LRRIg (Figure 3.4 A). Despite the low expression levels, a small-scale test purification of Amigo3 LRRIg was performed. Briefly, 100 ml of supernatant containing Amigo3 LRRIg was dialysed against PBS buffer and subsequently purified by Ni-NTA and gel-filtration (HR200) chromatography (Figure 3.4B left). Although the elution profile clearly shows a distinct peak (arrow), there are several other contaminants present (small peaks preceding the dominant peak). Based on the overlay of the elution profiles of Amigo1 LRRIg and Amigo3 LRRIg (Figure 3.4 B right) it was evident that Amigo3 LRRIg elutes at a similar place to Amigo1 LRRIg, showing the same shift of early elution. For this reason only the peak fraction (arrow) was collected and analysed by SDS-PAGE (Figure 3.4 C left). No differences between the reduced and non-reduced samples could be observed and although after gel-filtration Amigo3 LRRIg showed a higher degree of purity, there were still background proteins present. Overall, the protein was pure enough to continue with further experiments. As before, a western blot analysis on the purified protein using His-antibodies was performed to confirm its identity (Figure 3.4 C right). The total yield of the protein was lower than that for Amigo1 LRRIg, which was not surprising as the expression levels were considerably lower. After Ni-NTA purification, with 400 ml of supernatant, a total protein yield of 1.9 mg was obtained (~4.8 mg per/l) and after gel-filtration 78 µg of protein were purified. The high amount of protein found after Ni-NTA purification does not correspond with the finally purified protein amount. As the protein expression could not be detected on western blot and the elution profile of the gel-filtration column showed a lot of impurities, it is likely, that the OD reading of Amigo3 LRRIG was therefore falsely high, manipulated by unspecific bound proteins.

Figure 3.4: Expression analysis and Purification of Amigo3 LRRIg

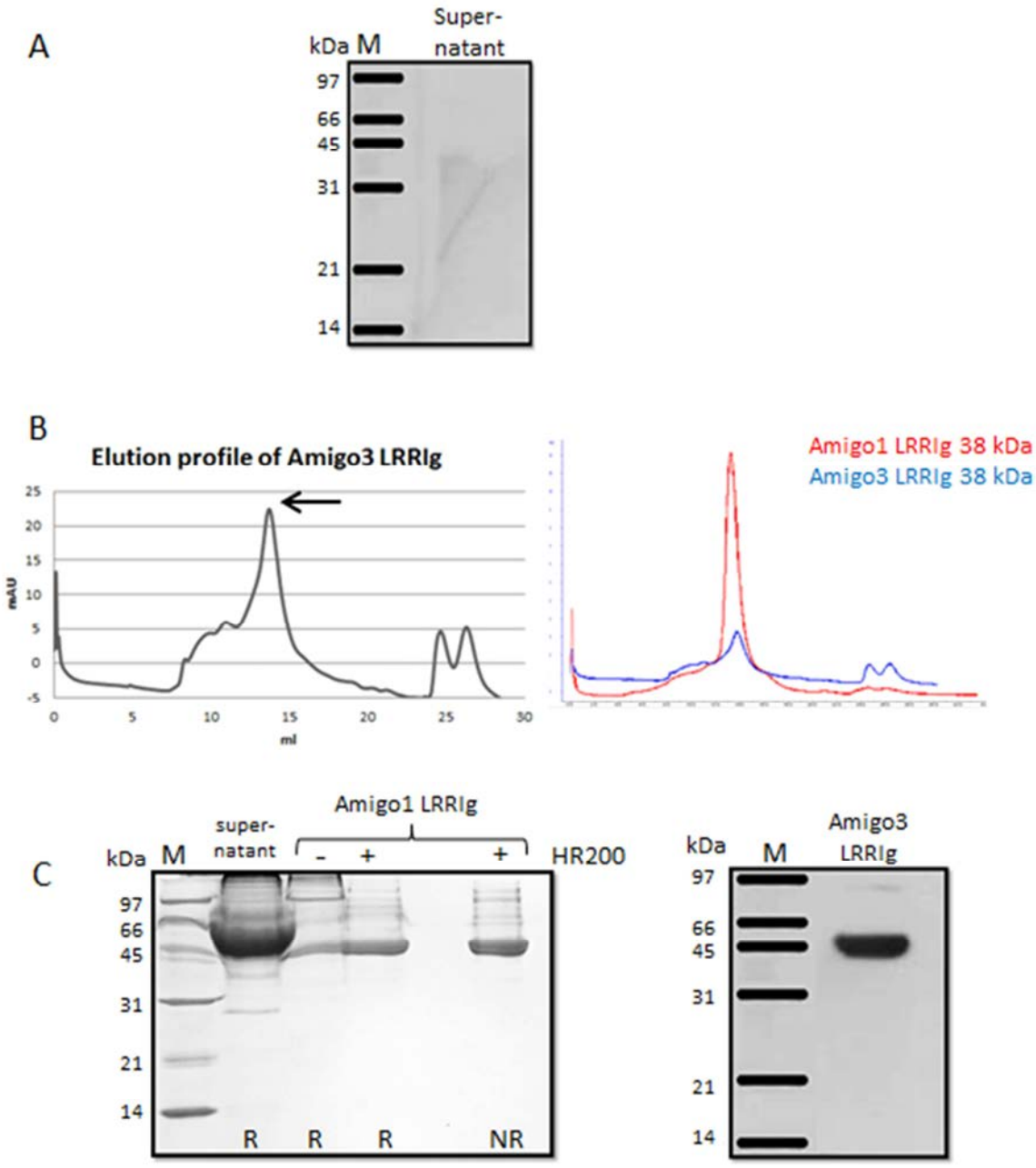

Figure 3.4: Expression and purification of Amigo-3 LRRIg. (A) Test expression of Amigo3 LRRIg. Western blot analysis of 20 µl S2 cells supernatant cells. (B) Test purification. 100 ml of supernatant was dialysed and purified with Ni-NTA and gel-filtration (elution profile of HR200 column; left). An overlay of Amigo1 LRRIg and Amigo3 LRRIg elution profiles (HR200 column, right). (C) Control of purification. 20 µl of supernatant and 8 µg of either Ni-bead purified protein (-HR200) or additionally gel filtered protein (+HR200) was loaded on a gel (in reducing (R) or non-reducing (NR) conditions, stained with Coomassie, left side). Western blot analysis of purified Amigo3 LRRIg (right).

3.4 Functional studies

3.4.1 Mass-spectrometry analysis of Amigo1 LRRIg and Amigo3 LRRIg

To confirm the identity of the purified proteins, western blots with His-antibodies had been performed. This is an indirect proof utilizing the His-tag of the fusion protein. To obtain direct evidence that Amigo1 LRR Ig and Amigo3 LRRIg were purified, bands from SDS-PAGE gel were excised and sent to be analysed by mass spectrometry (Helen Copper, Biosciences). For Amigo1 LRRIg a peptide coverage of 85% was observed and for Amigo3 LRRIg a peptide coverage of 90% of the cloned protein sequence could be achieved, thereby providing a direct confirmation of the identity of the purified proteins (Figure 3.5).

3.4.2 Deglycosylation of Amigo1 LRRIg and Amigo3 LRRIg

The expected sizes of Amigo1 LRRIg and Amigo3 LRRIg, calculated based on their primary amino acid sequence, were ~38 kDa. On SDS-PAGE the Amigo proteins migrated at a size corresponding to ~45 kDa. This led to the suggestion that these proteins may be glycosylated. To test this hypothesis Amigo1 and Amigo3 LRRIg were treated with the deglycosylation enzyme PNGase F (Figure 3.6 A). In the treated samples smaller bands (~40 kDa) appeared, resulting from the removal of the glycosyl-groups. The confirmed protein-glycosylation would explain the larger size of the proteins on SDS-PAGE.

3.4.3 Cross-linking of Amigo1 LRRIg and Amigo3 LRRIg

As noted earlier during gel-filtration both Amigo proteins eluted earlier from the column than expected for their size. This led to the suggestion that Amigo proteins may form dimers in solution. To address this, cross-linking experiments were performed. For these cross-linking experiments the Tris-buffer could not be used as it is a primary amine and would interfere with the cross-linking process, in which Lysines are covalently linked by the cross-linker. Therefore, Amigo1 LRRIg and Amigo3 LRRIg were purified in the presence of Hepes buffer pH 8.

Figure 3.5: Mass-Spectrometry data for Amigo1 LRRIg and Amgio3 LRRIg

Amigo1, human

MHPHRDPRGLWLLLPSLSLLLFEVARA// GRAVVSCPAACLCASNILSCSKQQLPNVPHS
LPSYTALLDLSHNNLSRLRAEWTPTRLTQLHSLLLSHNHLNFISSEAFSPVPNLRYLDLS
SNQLRTLDEFLFSDLQVLEVLLLYNNHIMAVDRCAFDDMAQLQKLYLSQNQISRFPLELV
KEGAKLPKLTLLDLSSNKLKNLPLPDLQKLPAWIKNGLYLHNNPLNCDCELYQLFSHWQY
RQLSSVMDFQEDLYCMNSKKLHNVFNLSFLNCGEYKERAWEAHLGDTLIIKCDTKQQGMT
KVWVTPSNERVLDEVTNGTVSVSKDGSLLFQQVQVEDGGVYTCYAMGETFNETLSVELKV
HNFTLHGHHDTLNT//AYTTLVGCILSVVLVLIYLYLTPCRCWCRGVEKPSSHQGDSLSS
SMLSTTPNHDPMAGGDKDDGFDRRVAFLEPAGPGQGQNGKLKPGNTLPVPEATGKGQRRM
SDPESVSSVFSDTPIVV

Amigo3, human

MTWLVLLGTLLCMLRVGLG//TPDSEGFPPRALHNCPYKCICAADLLSCTGLGLQDVPAE
LPAATADLDLSHNALQRLRPGWLAPLFQLRALHLDHNELDALGRGVFVNASGLRLLDLSS
NTLRALGRHDLDGLGALEKLLLFNNRLVHLDEHAFHGLRALSHLYLGCNELASFSFDHLH
GLSATHLLTLDLSSNRLGHISVPELAALPAFLKNGLYLHNNPLPCDCRLYHLLQRWHQRG
LSAVRDFAREYVCLAFKVPASRVRFFQHSRVFENCSSAPALGLERPEEHLYALVGRSLRL
YCNTSVPAMRIAWVSPQQELLRAPGSRDGSIAVLADGSLAIGNVQEQHAGLFVCLATGPR
LHHNQTHEYNVSVHFPRPEPEAFNT//GFTTLLGCAVGLVLVLLYLFAPPCRCCRRACRC
RRWPQTPSPLQELSAQSSVLSTTPPDAPSRKASVHKHVVFLEPGRRGLNGRVQLAVAEEF
DLYNPGGLQLKAGSESASSIGSEGPMTT

Figure 3.5: Mass-Spectrometry data for Amigo1 LRRIg and Amgio3 LRRIg. Samples of Amigo1 LRRIg and Amigo3 LRRIg were excised from a a SDS-PAGE and sent for analysis by mass-spectrometry. The whole protein sequences for Amigo1 and Amigo3 are shown. The relevant protein sequences, as cloned, are separated by // and marked with yellow. The peptides, which were detected by mass-spectrometry, are indicated in green. For Amigo1 LRRIg and Amigo 3 LRRIg, a coverage of 85 and 90 % was achieved.

Figure 3.6: Crosslinking and Deglycosylation of Amigo1 and Amigo3 LRRIg

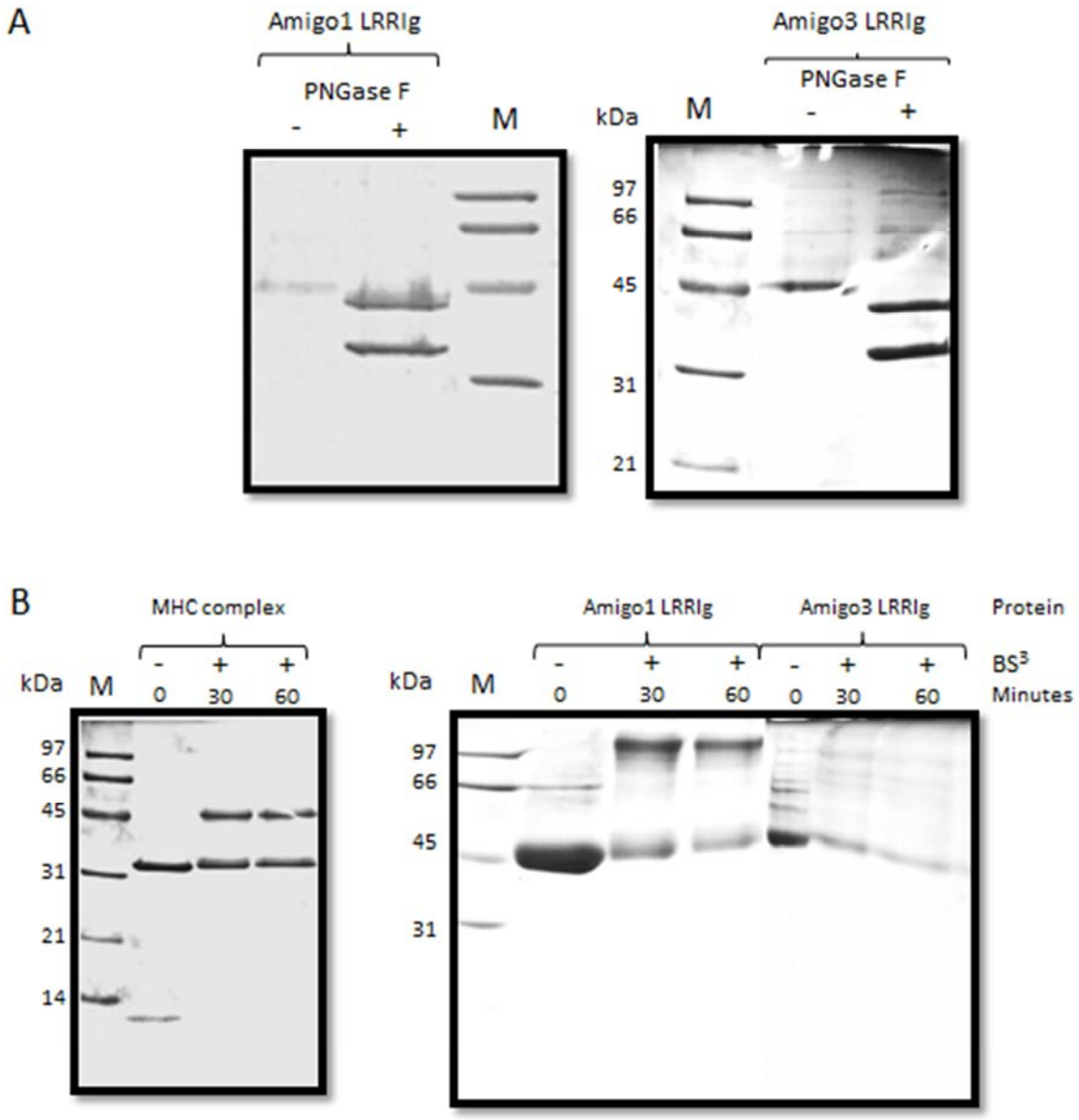

Figure 3.6: Deglycosylation and cross-linking of Amigo1 and Amigo3 LRRIg. (A) Removal of Glycosyl-groups of protein. Amigo1 LRRIg and Amigo3 LRRIg were treated with PNGase F, which cleaves protein glycosyl-groups. Samples were loaded on a gel and stained with Coomassie. (B) Cross-linking analysis for dimerisation. MHC complex (left) Amigo1 LRRIg, Amigo3 LRRIg (right) were treated with BS^3 and analysed by SDS-PAGE. Samples were taken at indicated time points

.

The MHC complex (45 kDa, composed of a heavy chain (33kDa) and a light chain (12 kDa)) was selected as a positive control for the cross-linking experiments. Initial cross-linking trials with DMP(DimethylPimelidate) failed to cross-link either the MHC complex or the Amigo-proteins (data not shown). Analysis of the MHC protein structure revealed that the lysines were at least 10 Å apart and that the spacer arm of DMP (9.2 Å) was too short to connect them. For this reason two cross-linkers with longer spacer arms (BS^3=11.4 Å and SEGS=16 Å) were tested. Both cross-linkers worked and the results for BS^3 shown in Figure 3.6 B. Following the cross-linking experiment with the MHC complex, a band around 45kDa is observed (Figure 3.6 B left). For Amigo1 LRRIg, the negative control displays a native 45kDa band, while in the cross-linked samples a bigger ~100 kDa band is observed (Figure 3.6 B right). This suggests that Amigo1 LRRIg can exist as a dimer in solution and porvides a likely explanation for the early shifts in elution during gel filtration chromatography. In contrast, for Amigo3 LRRIg, no differences in the negative control or the cross-linked samples could be observed (Figure 3.6 B right).

3.4.4 BIAcore binding analysis of Amigo1 LRRIg and Amigo3 LRRIg

To prove if Amigo proteins may substitute for Lingo1 in forming a ternary complex with p75 and NgR, direct binding of Amigo proteins to NgR or p75 was tested by BIAcore. Briefly, NgR-Fc and p75-Fc were coupled to the surface of the sensor chip and the Amigo proteins in Tris-buffer were injected over the flow cells. Ni-NTA purified Amigo protein samples, were initially tested (Figure 3.7 A and C). However, these samples were adhering non-specifically to the flow-cell surface and therefore could not be used. Amigo protein samples that were additionally gel-filtrated after the Ni-NTA purification, were available, although at a lower concentration. Samples purified by gel filtration did not stick as before (Figure 3.7 B, D and E), but the results were still inconclusive. Certainly a stable protein-protein interaction analogous to that proposed between LINGO-1 and NgR (Mosyak, Wood et al. 2006) could be excluded, as the off-rate was too fast. At present, based on the binding data a weak protein-protein interaction between the Amigo proteins and NgR-Fc, involving a fast off-rate, cannot be excluded. For example, during the binding phase, for Amigo1 LRRIg (0.48 mg/ml) a response of 20 units to the NgR-Fc (Figure 3.7 B) was observed. In comparison for Amigo3 LRRIg (0.4 mg/ml) a larger binding response of 75 units were evident (Figure 3.7 D). Also,

injection of lower concentrations of Amigo3 LRRIg (0.1 mg/ml) over a flow cell with NgR-Fc led to a smaller binding response of 20 units (Figure 3.7 E). Interestingly, in the flow-cell coated with NgR-Fc and p75-Fc, a small binding response was visible (40 units for Amigo3 LRRIg 0.4 mg/ml (Figure 3.7 D), 10 units for Amigo3 LRRIg 0.1 mg/ml (Figure 3.7 E)). However, in the flow-cell that was coated with p75-Fc, no binding response was visible for either Amigo proteins. The buffer control (Figure 3.7 F) demonstrated that the flow-cells were coated with similar levels of protein on their surfaces. Although such signals are relatively low compared to the level of NgR-Fc and p75-Fc immobilised, these results do not rule a weak protein-protein interactions between the tested Amigo proteins and NgR out. However, further experiments are needed to unequivocally prove that Amigo proteins bind to NgR and p75.

3.4.5 Crystallisation Trials of Amigo1 LRRIg

To determine the three dimensional structure of the Amigo proteins by X-ray crystallography, protein crystals were needed. For the crystallisation trials were limited to Amigo1 LRRIg as it was available in suitable quantities and sufficiently pure. To grow protein crystals the protein molecules in solution need to specifically interact with each other. The components in a crystallization solution (buffer, salt and precipitant) support this process, but vary for each protein. To identify the optimal crystallization solution for Amigo1 LRRIg, three commercial screens were tested on a small scale using the "Hanging Drop vapour diffusion method". Following the initial crystallisation screening trials, three conditions yielded possible signs of crystals after one week (Figure 3.8 A). The trials were repeated on a small-scale with the most promising condition (JCSG$^+$ 1.20; 0.2 M $MgCl_2$, 0.1 M Tris pH 8, 10% PEG 8000). In most of the drops multiple crystals were observed, of a size of ~40x40 microns (Figure 3.7 B left and middle), while in the negative controls, in which the protein solution was replaced by crystallization buffer, no crystals were observed (Figure 3.8 B right). These crystals were too small for X-ray diffraction experiments, as typically a minimum size of ~100x100 microns is needed. The crystallization process with the identified condition was therefore scaled up. However, initial large scale attempts, using the last amounts of purified Amigo1 LRRIg protein, failed to yield crystals with only aggregates found in the drops. In order to optimise the crystallization process different variations of the

methods were tested. (I) The protein concentration of Amgio1 LRRIg (normally 10mg/ml) was varied between 9 mg/ml and 7 mg/ml as well the amount of PEG 8K (from 10% to 7.5%). (II) Protein:crystallisation buffer drop sizes were varied from 100+100 nl to 200+200nl and 400+400nl. (III) the drop ratio of protein solution and crystallization buffer was varied (from 1:1 to 1:2 and 1:3). (IV) "sitting drop vapour diffusion method", in which the drops were place on a bridge over the buffer reservoir, was tested. (V) The large scale up was repeated using commercial conditions rather than using the home-made condition. These modifications, finally using the commercial condition and using a new batch of purified Amigo 1 LRRIg protein, led to the growth of crystals after one week, which were large enough to attempt initial X-ray diffraction experiments (Figure 3.8 C).

Figure 3.7: BIAcore binding analysis of Amigo1 LRRIg and Amigo3 LRRIg

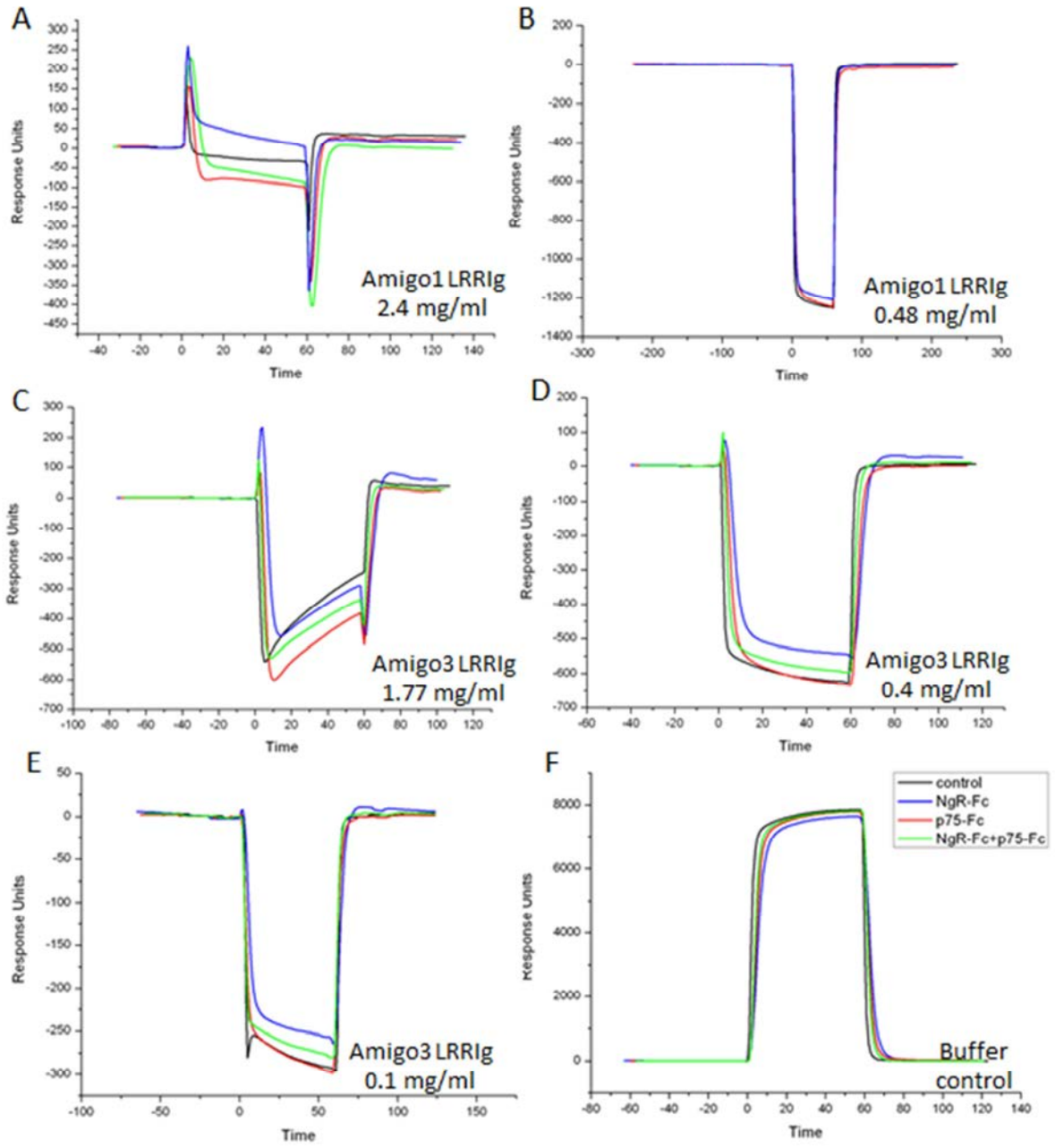

Figure 3.7: BIAcore binding analysis of Amigo1 LRRIg and Amigo3 LRRIg.
Flow cells, coated either with NgR-Fc (blue), p75-Fc (red), NgR-Fc and p75-Fc (green) or Fc-Antibody alone (negative control, black) were injected with
Ni-NTA purified Amigo1 LRRIg.
Ni-NTA purified, gel-filtrated Amigo1 LRRIg.
Ni-NTA purified Amigo3 LRRIg.
Ni-NTA purified, gel-filtrated Amigo3 LRRIg.
Ni-NTA purified, gel-filtrated Amigo3 LRRIg.
Hepes buffer.

Figure 3.8: Crystallization trials for Amigo1 LRRIg

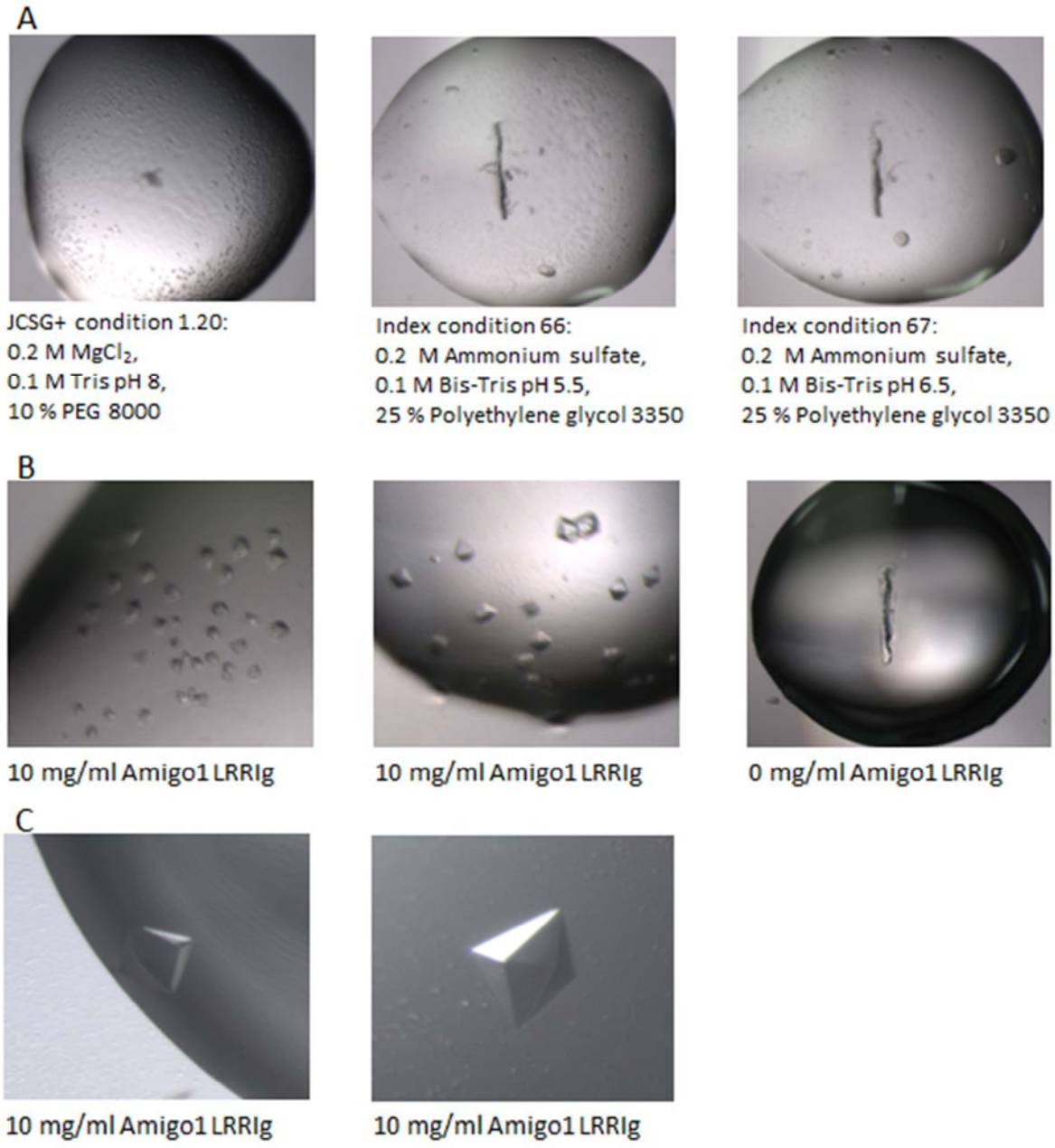

Figure 3.8: Crystallization trials for Amgio1 LRRIg. (A) Crystallisation conditions that have yielded Amigo1 LRRIg crystals using the hanging drop vapour diffusion method. (B) Small-scale trials with JCSG+ condition 1:20. Crystals of Amigo1 LRRIg (40x40 microns) were grown (left and middle) but no crystals were observed in the negative control (right). (C) Large-scale trials with JCSG+ condition 1:20 with 1:1 (left) and 1:3 (right) ratio drops (protein:crystallisation buffer). The crystals reached a size of ~100x100 microns.

4. Discussion

In the CNS only limited regeneration is observed following injury, partly resulting from the action of myelin derived inhibitors (MAG, Nogo, OMgp), which all bind to the Nogo-receptor complex, consisting of NgR, p75 and Lingo1 (Filbin 2008). Lingo1 is one member of a large group of CNS enriched membrane proteins, with a LRR and an Ig domain in their ectodomain. Other members of this LRR-Ig protein family include the Amigo-proteins, which have previously been described in the context of neuronal development and survival (Kuja-Panula, Kiiltomaki et al. 2003; Ono, Sekino-Suzuki et al. 2003). Little is known about the molecular mechanisms governing Amigo protein function within the CNS. Recent microarray experiments showed up-regulation of specific Amigo proteins following CNS injury, suggesting that these LRR-Ig folded proteins could be relevant to the CNS injury response and/or regenerative pathways (M. Douglas, personal communication). An interaction of the Amigo-proteins with NgR and p75 could be demonstrated by Co-immuoprecipitation studies (M. Douglas, personal communication). This data suggested that the Amigo-proteins may substitute for Lingo1 in forming a ternary NgR complex. In this project this hypothesis was examined using a combination of biochemical, binding and structural approaches.

4.1 Purification of Amigo ectodomains

To gain an in-depth understanding of Amigo function, the entire ectodomains of Amigo proteins 1, 2 and 3 (LRR and the Ig domain) as well as a shorter ectodomain (containing only the LRR domain) should be expressed in recombinant form. However, due to time constraints for this project three constructs were cloned. These include the short ectodomain of Amigo1 (Amigo1 LRR), and the entire ectodomains of Amigo1 (Amigo LRRIg) and Amigo3 (Amigo3 LRRIg). Initially, these constructs were expressed and purified for subsequent functional and structural analysis. The results varied significantly for each construct. Amigo1 LRR showed very good levels of expression based on the western blot analysis of the S2 supernatant. However, following Ni-NTA purification it was found to be impure containing a number of unspecified contaminating proteins and as a result the purification conditions were modified to increase the purity of the protein. The final

optimised purification procedure for Amigo1 LRR- consisted of increasing the Imidazole concentration (from 10-20mM) in the wash step (to remove non-specific proteins) followed by gel filtration chromatography. Despite producing pure Amigo1 LRR, much protein was lost such that further studies could not be carried out. One potentiallly interesting aspect would be to examine whether the other Amigo proteins (2 and 3) with similarly truncated ectodomains behave in a similar manner to Amigo1 LRR. If they behave in a comparable way, it may suggest that the Amigo LRR domains on their own are not very stable and increasingly prone to forming aggregates and unspecific interactions. To overcome this problem it may be worth re-engineering the protein and extending the flanking regions or adding another fusion tag (eg. GST). If this does not work, a slightly different approach could examine the structural properties of an ectodomain lacking the LRR domain.

In contrast, the whole ectodomain of Amigo1 was stably expressed and could be easily purified with high yields of pure protein.

Intriguingly, Western blot analysis of Amigo3 LRRIg expression showed no signal, although other signals on the same blot were clearly visible. The membrane when stained with Ponceau-Red revealed that adequate material was loaded and that the blotting had worked. This may suggest that overall expression levels of Amigo3 LRRIg are low. This finding is in contrast to the OD reading performed after Ni-NTA purification of 400 ml of supernatant, which revealed a yield of ~2 mg of protein. An explanation would be that the protein was very impure and falsified the measurement. The elution profiles of the gel-filtration columns support this, as they revealed a much unspecific protein attached to Amigo3 LRRIg. The final yield of protein was further reduced once impurities were separated from the Ni-NTA purified protein sample by gel filtration chromatography. Nevertheless, there was sufficient Amigo3 LRRIg protein available for functional studies.

It was observed, that the protein was not stable in PBS buffer and formed aggregates or precipitates after thawing. The pH of PBS is close to the predicted isoelectric points of the Amigo proteins, leaving them without charge and therefore possibly unstable in solution. For this reason all Amigo proteins were transferred into Tris-buffer with a higher pH.

4.2 Functional Analysis of Amigo1 LRRIg and Amigo3 LRRIg

During the purification process it was evident that the Amigo proteins migrated aberrantly on a SDS-PAGE gel. Based on their primary amino sequences a molecular weight of ~38 kDa was calculated, but on the SDS-PAGE gel bands corresponding to ~45 kDa were observed. This led to the suggestion that the Amigo LRRIg proteins may be post-translationally modified by glycosylation. To test this Amigo1 and Amigo3 LRRIg were treated with a deglycosylation enzyme, which proved that these proteins were glycosylated.

Another striking observation during purification was that Amigo proteins eluted earlier than expected from the gel filtration column. This effect could have been due to the overall shape, which beside the size can influence the protein elution profile. Alternatively Amigo LRRIg proteins may exist as oligomers in solution. This would be consistent with structural studies of Lingo1, which suggested that Lingo1 forms tetramers in solution and confirmed it by cross-linking experiments (Mosyak, Wood et al. 2006). Although the non-reduced samples on the SDS-PAGE gel run as monomers, it could not be ruled out that they exist as oligomers in solution. To further clarify this issue, cross-linking analyses was performed on the Amigo 1 and 3 LRRIg proteins. Three different cross-linkers, with different length spacer-arms were used. After the initial failed attempts with DMP (9.2 Å spacer arm), cross-linking was successfully performed using the reagents BS^3 and Sulfo-EGF (11.2 and 16 Å spacer-arms) including the positive control (MHC complex), indicating that the method was working. For Amigo1 LRRIg, a cross-linked band corresponding to ~100 kDa was visible, suggesting that Amigo1 LRRIg can form high order oligomers (most probably dimers) in solution.

In contrast, for Amigo3 LRRIg no evidence for dimerisation could be observed in all attempted cross-linking experiments. It is therefore possible that Amigo3 LRRIg does not oligomerize. However, Amigo3 LRRIg eluted similarly to Amigo1 LRRIg upon gel filtration, and so this lack of evidence for a oligomer should be treated with caution. One limitation to this result is that limited protein of lower purity was available for the cross-linking experiment (4 µg instead of the recommended 5-10 µg), which may have had an effect on the final result. In addition, such cross-linking approaches rely on the presence of appropriate functional groups on Amigo 3 LRRIg, which may have been absent. Therefore, the cross-linking experiments for Amigo3 LRRIg need to be repeated, preferentially with

more and purer protein, and possibly with alternative cross-linkers, before a more conclusive statement can be made. In either case for the future a more definitive answer on the oligomerisation status of Amigo LRRIg proteins could be provided by analytical ultracentrifugation.

BIAcore technology was used to examine whether Amigo proteins can directly bind to NgR or p75 and form a ternary complex, as was demonstrated for Lingo1 (Mosyak, Wood et al. 2006). This involved injecting purified Amigo proteins over flow cells coated with NgR-Fc and p75-Fc. Although these results proved inconclusive, a stable protein-protein interaction could clearly be ruled out, as the off-rate was too rapid. This may not be surprising since for NgR and p75 to assemble with a Amigo protein a weak interaction may be sufficient, as they are all membrane surface proteins and therefore in close contact to each other. During the injection phase a small binding response was evident for the flow cells, coated with NgR-Fc. For the flow cells coated with p75, however, no binding at all could be demonstrated. There are several points to take into consideration before repeating the BIAcore experiments. Firstly the flow cells were coated with slightly different amounts of proteins. This would not be a problem for a high affinity protein interaction, but could make a significant difference in the detection of weak interactions. Secondly, the coating of flow cells with Fc-antibodies could have placed the NgR and p75 in a sterically unfavourable position, thus preventing the Amigo proteins from binding optimally. Alternatively, the NgR-Fc and p75-Fc proteins may be functionally inactive. To confirm or to rule out a weak interaction between the three proteins a modified protocol could involve injecting Amigo proteins over NgR and p75 immobilised on streptavidin rather than using Fc proteins. This strategy might conceivably counteract the steric hindrance related issue. Also, to rule out the possibilities that the putative Fc ligands are inactive, a positive control is required for the BIAcore experiments. In this case the Lingo-1 ectodomain would be a good candidate, as previous studies have demonstrated direct binding between Lingo-1 and NgR-Fc (Mosyak, Wood et al. 2006). Finally, the Tris buffer provided a negative buffer signal which is less favourable for detecting weak interactions. It may be more desirable to use a different buffer that gives a positive buffer signal, as smaller response differences are better detected in buffers that yield a positive signal.

Preliminary experiments designed to produce crystals for structural studies of Amigo1 LRRIg were performed. Initial screening trials using the mosquito nano-litre crystallisation robot identified several conditions that yielded potential crystal hits. The best hit was then optimised and scaled up. The crystallisation trials were successful with one condition yielding crystals that are sufficient in size for subsequent X-ray diffraction experiments. Similar tests will be performed for the other Amigo proteins, when sufficient amounts of purified proteins are available.

4.3 Concluding remarks

The aim of the project was to examine whether Amigo proteins could substitute for Lingo1 and directly bind to NgR and p75 and form a ternary complex. As discussed above Amigo1 LRRIg and Amigo3 LRRIg were expressed and purified. Currently, Amigo2 LRRIg and Lingo1 LRRIg are at the cloning stage and will be expressed, purified and tested to gain further insights into the function of Amigo family members. However, based on this project it has not been possible to conclude whether the Amigo proteins can substitute for Lingo1 in forming the NgR complex and further studies are needed.

A second aim was to initiate structural studies for Amigo proteins to determine their three dimensional structure. For Amigo1 LRRIg considerable progress has been made with the growth of crystals that are sufficient in size for preliminary X-ray diffraction experiments. In further studies in this field one important consideration is the potential complexity of the Nogo-receptor complex. This complexity results from the fact that two more isoforms of the Nogo-receptor, namely NgR2 and NgR3, exist, which have overlapping but distinct distributions in the matured CNS (Venkatesh, Chivatakarn et al. 2005; Chivatakarn, Kaneko et al. 2007). Their potential importance is seen with the observation that the loss of NgR1 is not sufficient for attenuating MAG inhibition (Venkatesh, Chivatakarn et al. 2007). It would also be possible that the Amigo proteins interact with NgR2 or NgR3 rarther than NgR1, which was examined here. Thus future binding experiments should include testing whether Amigo proteins bind to these isoforms.

It is therefore possible, that the formation of the NgR complex, and resultant functional properties is far more complicated than currently appreciated. It is likely that this area of research will continue to be the subject of intense study for many years to come.

References Project I

Ansari, K. I., B. P. Mishra, et al. (2009). "MLL histone methylases in gene expression, hormone signaling and cell cycle." Front Biosci **14**: 3483-95.

Argiropoulos, B. and R. K. Humphries (2007). "Hox genes in hematopoiesis and leukemogenesis." Oncogene **26**(47): 6766-76.

Barber, B. A. and M. Rastegar (2010). "Epigenetic control of Hox genes during neurogenesis, development, and disease." Ann Anat **192**(5): 261-74.

Berger, S. L. (2007). "The complex language of chromatin regulation during transcription." Nature **447**(7143): 407-12.

Berger, S. L., T. Kouzarides, et al. (2009). "An operational definition of epigenetics." Genes Dev **23**(7): 781-3.

Chen, J., D. A. Santillan, et al. (2008). "Loss of MLL PHD finger 3 is necessary for MLL-ENL-induced hematopoietic stem cell immortalization." Cancer Res **68**(15): 6199-207.

Daniel, J. A., M. G. Pray-Grant, et al. (2005). "Effector proteins for methylated histones: an expanding family." Cell Cycle **4**(7): 919-26.

de la Cruz, X., S. Lois, et al. (2005). "Do protein motifs read the histone code?" Bioessays **27**(2): 164-75.

Delcuve, G. P., M. Rastegar, et al. (2009). "Epigenetic control." J Cell Physiol **219**(2): 243-50.

Dorigo, B., T. Schalch, et al. (2004). "Nucleosome arrays reveal the two-start organization of the chromatin fiber." Science **306**(5701): 1571-3.

Dou, Y., T. A. Milne, et al. (2005). "Physical association and coordinate function of the H3 K4 methyltransferase MLL1 and the H4 K16 acetyltransferase MOF." Cell **121**(6): 873-85.

Drobic, B., B. Perez-Cadahia, et al. (2010). "Promoter chromatin remodeling of immediate-early genes is mediated through H3 phosphorylation at either serine 28 or 10 by the MSK1 multi-protein complex." Nucleic Acids Res **38**(10): 3196-208.

Dyson, M. H., S. Thomson, et al. (2005). "MAP kinase-mediated phosphorylation of distinct pools of histone H3 at S10 or S28 via mitogen- and stress-activated kinase 1/2." J Cell Sci **118**(Pt 10): 2247-59.

Edmunds, J. W. and L. C. Mahadevan (2004). "MAP kinases as structural adaptors and enzymatic activators in transcription complexes." J Cell Sci **117**(Pt 17): 3715-23.

Felsenfeld, G. and M. Groudine (2003). "Controlling the double helix." Nature **421**(6921): 448-53.

Fischle, W. (2008). "Talk is cheap--cross-talk in establishment, maintenance, and readout of chromatin modifications." Genes Dev **22**(24): 3375-82.

Franklin, T. B. and I. M. Mansuy (2010). "Epigenetic inheritance in mammals: evidence for the impact of adverse environmental effects." Neurobiol Dis **39**(1): 61-5.

Haberland, M., A. Johnson, et al. (2009). "Genetic dissection of histone deacetylase requirement in tumor cells." Proc Natl Acad Sci U S A **106**(19): 7751-5.

Hansen, J. C., J. K. Nyborg, et al. (2010). "Histone chaperones, histone acetylation, and the fluidity of the chromogenome." J Cell Physiol **224**(2): 289-99.

Henikoff, S. (2008). "Nucleosome destabilization in the epigenetic regulation of gene expression." Nat Rev Genet **9**(1): 15-26.

Hueber, S. D., G. F. Weiller, et al. (2010). "Improving Hox protein classification across the major model organisms." PLoS One **5**(5): e10820.

Jaenisch, R. and A. Bird (2003). "Epigenetic regulation of gene expression: how the genome integrates intrinsic and environmental signals." Nat Genet **33 Suppl**: 245-54.

Jenuwein, T. and C. D. Allis (2001). "Translating the histone code." Science **293**(5532): 1074-80.

Khorasanizadeh, S. (2004). "The nucleosome: from genomic organization to genomic regulation." Cell **116**(2): 259-72.

Kouzarides, T. (2007). "Chromatin modifications and their function." Cell **128**(4): 693-705.

Latham, J. A. and S. Y. Dent (2007). "Cross-regulation of histone modifications." Nat Struct Mol Biol **14**(11): 1017-1024.

Lau, P. N. and P. Cheung "Histone code pathway involving H3 S28 phosphorylation and K27 acetylation activates transcription and antagonizes polycomb silencing." Proc Natl Acad Sci U S A **108**(7): 2801-6.

Lee, B. M. and L. C. Mahadevan (2009). "Stability of histone modifications across mammalian genomes: implications for 'epigenetic' marking." J Cell Biochem **108**(1): 22-34.

Luger, K., A. W. Mader, et al. (1997). "Crystal structure of the nucleosome core particle at 2.8 A resolution." Nature **389**(6648): 251-60.

Macdonald, N., J. P. Welburn, et al. (2005). "Molecular basis for the recognition of phosphorylated and phosphoacetylated histone h3 by 14-3-3." Mol Cell **20**(2): 199-211.

McGinnis, W., R. L. Garber, et al. (1984). "A homologous protein-coding sequence in Drosophila homeotic genes and its conservation in other metazoans." Cell **37**(2): 403-8.

Mellor, J. (2006). "Dynamic nucleosomes and gene transcription." Trends Genet **22**(6): 320-9.

Mellor, J. (2006). "It takes a PHD to read the histone code." Cell **126**(1): 22-4.

Milne, T. A., J. Kim, et al. (2002). "Multiple interactions recruit MLL1 and MLL1 fusion proteins to the HOXA9 locus in leukemogenesis." Mol Cell **38**(6): 853-63.

Mujtaba, S., L. Zeng, et al. (2007). "Structure and acetyl-lysine recognition of the bromodomain." Oncogene **26**(37): 5521-7.

Nightingale, K. P., S. Gendreizig, et al. (2007). "Cross-talk between histone modifications in response to histone deacetylase inhibitors: MLL4 links histone H3 acetylation and histone H3K4 methylation." J Biol Chem **282**(7): 4408-16.

Pinto do, O. P., A. Kolterud, et al. (1998). "Expression of the LIM-homeobox gene LH2 generates immortalized steel factor-dependent multipotent hematopoietic precursors." Embo J **17**(19): 5744-56.

Ruthenburg, A. J., W. Wang, et al. (2006). "Histone H3 recognition and presentation by the WDR5 module of the MLL1 complex." Nat Struct Mol Biol **13**(8): 704-12.

Schones, D. E., K. Cui, et al. (2008). "Dynamic regulation of nucleosome positioning in the human genome." Cell **132**(5): 887-98.

Slany, R. K. (2005). "When epigenetics kills: MLL fusion proteins in leukemia." Hematol Oncol **23**(1): 1-9.

Soloaga, A., S. Thomson, et al. (2003). "MSK2 and MSK1 mediate the mitogen- and stress-induced phosphorylation of histone H3 and HMG-14." Embo J **22**(11): 2788-97.

Taverna, S. D., H. Li, et al. (2007). "How chromatin-binding modules interpret histone modifications: lessons from professional pocket pickers." Nat Struct Mol Biol **14**(11): 1025-40.

Thomson, S., A. L. Clayton, et al. (1999). "The nucleosomal response associated with immediate-early gene induction is mediated via alternative MAP kinase cascades: MSK1 as a potential histone H3/HMG-14 kinase." Embo J **18**(17): 4779-93.

Turner, B. M. (2002). "Cellular memory and the histone code." Cell **111**(3): 285-91.

Turner, B. M. (2005). "Reading signals on the nucleosome with a new nomenclature for modified histones." Nat Struct Mol Biol **12**(2): 110-2.

Widmann, C., S. Gibson, et al. (1999). "Mitogen-activated protein kinase: conservation of a three-kinase module from yeast to human." Physiol Rev **79**(1): 143-80.

Woodcock, C. L. and R. P. Ghosh (2011). "Chromatin higher-order structure and dynamics." Cold Spring Harb Perspect Biol **2**(5): a000596.

Wysocka, J., T. Swigut, et al. (2006). "A PHD finger of NURF couples histone H3 lysine 4 trimethylation with chromatin remodelling." Nature **442**(7098): 86-90.

Yokoyama, A., T. C. Somervaille, et al. (2005). "The menin tumor suppressor protein is an essential oncogenic cofactor for MLL-associated leukemogenesis." Cell **123**(2): 207-18.

Zheng, C. and J. J. Hayes (2003). "Intra- and inter-nucleosomal protein-DNA interactions of the core histone tail domains in a model system." J Biol Chem **278**(26): 24217-24.

References Project II

Bella, J., K. L. Hindle, et al. (2008). "The leucine-rich repeat structure." Cell Mol Life Sci **65**(15): 2307-2333.

Benson, D. L., D. R. Colman, et al. (2001). "Molecules, maps and synapse specificity." Nat Rev Neurosci **2**(12): 899-909.

Chen, Y., S. Aulia, et al. (2006). "AMIGO and friends: an emerging family of brain-enriched, neuronal growth modulating, type I transmembrane proteins with leucine-rich repeats (LRR) and cell adhesion molecule motifs." Brain Res Rev **51**(2): 265-274.

Chivatakarn, O., S. Kaneko, et al. (2007). "The Nogo-66 receptor NgR1 is required only for the acute growth cone-collapsing but not the chronic growth-inhibitory actions of myelin inhibitors." J Neurosci **27**(27): 7117-7124.

de Wit, J., W. Hong, et al. (2010). "Role of Leucine-Rich Repeat Proteins in the Development and Function of Neural Circuits." Annu Rev Cell Dev Biol.

Fournier, A. E., T. GrandPre, et al. (2001). "Identification of a receptor mediating Nogo-66 inhibition of axonal regeneration." Nature **409**(6818): 341-346.

Filbin, M. T. (2008). "PirB, a second receptor for the myelin inhibitors of axonal regeneration Nogo66, MAG, and OMgp: implications for regeneration in vivo." Neuron **60**(5): 740-742.

Giger, R. J., E. R. Hollis, 2nd, et al. (2010). "Guidance molecules in axon regeneration." Cold Spring Harb Perspect Biol **2**(7): a001867.

He, X. L., J. F. Bazan, et al. (2003). "Structure of the Nogo receptor ectodomain: a recognition module implicated in myelin inhibition." Neuron **38**(2): 177-185.

Inoue, H., L. Lin, et al. (2007). "Inhibition of the leucine-rich repeat protein LINGO-1 enhances survival, structure, and function of dopaminergic neurons in Parkinson's disease models." Proc Natl Acad Sci U S A **104**(36): 14430-14435

Ji, B., M. Li, et al. (2006). "LINGO-1 antagonist promotes functional recovery and axonal sprouting after spinal cord injury." Mol Cell Neurosci **33**(3): 311-320.

Kobe, B. and A. V. Kajava (2001). "The leucine-rich repeat as a protein recognition motif." Curr Opin Struct Biol **11**(6): 725-732.

Kuja-Panula, J., M. Kiiltomaki, et al. (2003). "AMIGO, a transmembrane protein implicated in axon tract development, defines a novel protein family with leucine-rich repeats." J Cell Biol **160**(6): 963-973.

Lee, X., Z. Yang, et al. (2007). "NGF regulates the expression of axonal LINGO-1 to inhibit oligodendrocyte differentiation and myelination." J Neurosci **27**(1): 220-225.

Llorens, F., V. Gil, et al. (2008). "Developmental analysis of Lingo-1/Lern1 protein expression in the mouse brain: interaction of its intracellular domain with Myt1l." Dev Neurobiol **68**(4): 521-541.

McDonald, C. L., C. Bandtlow, et al. (2011). "Targeting the Nogo receptor complex in diseases of the central nervous system." Curr Med Chem **18**(2): 234-244.

Mi, S., X. Lee, et al. (2004). "LINGO-1 is a component of the Nogo-66 receptor/p75 signaling complex." Nat Neurosci **7**(3): 221-228.

Mi, S., R. H. Miller, et al. (2005). "LINGO-1 negatively regulates myelination by oligodendrocytes." Nat Neurosci **8**(6): 745-751.

Mi, S., R. H. Miller, et al. (2009). "Promotion of central nervous system remyelination by induced differentiation of oligodendrocyte precursor cells." Ann Neurol **65**(3): 304-315.

Mi, S., A. Sandrock, et al. (2008). "LINGO-1 and its role in CNS repair." Int J Biochem Cell Biol **40**(10): 1971-1978.

Mosyak, L., A. Wood, et al. (2006). "The structure of the Lingo-1 ectodomain, a module implicated in central nervous system repair inhibition." J Biol Chem **281**(47): 36378-36390.

Ono, T., N. Sekino-Suzuki, et al. (2003). "Alivin 1, a novel neuronal activity-dependent gene, inhibits apoptosis and promotes survival of cerebellar granule neurons." J Neurosci **23**(13): 5887-5896.

Park, J. B., G. Yiu, et al. (2005). "A TNF receptor family member, TROY, is a coreceptor with Nogo receptor in mediating the inhibitory activity of myelin inhibitors." Neuron **45**(3): 345-351.

Pernet, V., S. Joly, et al. (2008). "Nogo-A and myelin-associated glycoprotein differently regulate oligodendrocyte maturation and myelin formation." J Neurosci **28**(29): 7435-7444.

Schmidt, A. and A. Hall (2002). "Guanine nucleotide exchange factors for Rho GTPases: turning on the switch." Genes Dev **16**(13): 1587-1609.

Schuster, J. M. and P. S. Nelson (2000). "Toll receptors: an expanding role in our understanding of human disease." J Leukoc Biol **67**(6): 767-773.

Venkatesh, K., O. Chivatakarn, et al. (2005). "The Nogo-66 receptor homolog NgR2 is a sialic acid-dependent receptor selective for myelin-associated glycoprotein." J Neurosci **25**(4): 808-822.

Venkatesh, K., O. Chivatakarn, et al. (2007). "Molecular dissection of the myelin-associated glycoprotein receptor complex reveals cell type-specific mechanisms for neurite outgrowth inhibition." J Cell Biol **177**(3): 393-39

Wang, K. C., J. A. Kim, et al. (2002). "P75 interacts with the Nogo receptor as a co-receptor for Nogo, MAG and OMgp." Nature **420**(6911): 74-78.

Yamashita, T., M. Fujitani, et al. (2005). "Multiple signals regulate axon regeneration through the Nogo receptor complex." Mol Neurobiol **32**(2): 105-111.

Yiu, G. and Z. He (2006). "Glial inhibition of CNS axon regeneration." Nat Rev Neurosci **7**(8): 617-627.

Zhao, X. H., W. L. Jin, et al. (2007). "An in vitro study on the involvement of LINGO-1 and Rho GTPases in Nogo-A regulated differentiation of oligodendrocyte precursor cells." Mol Cell Neurosci **36**(2): 260-269.